AN OPTO-ELECTRONIC SOIL PROFILE METER

by

Javad Khorashahi

Thesis submitted to the Faculty of the

Virginia Polytechnic Institute and State University

in partial fulfillment of the requirements for the degree of

Master of Science

in

Agricultural Engineering

APPROVED:

Dr. Richard K. Byler, Chairman

Dr. T. A. Dillaha

Dr. J. V. Perumpral

June 1986

Blacksburg, Virginia

AN OPTO-ELECTRONIC SOIL PROFILE METER

by

Javad Khorashahi

Committee Chairman, Dr. R. K. Byler

Agricultural Engineering Department

(ABSTRACT)

A mechanical, non-contact soil profile meter was developed to measure soil elevations before and after an artificial rainfall for erosion studies. The design goals were to measure the heights of the soil in a 1.5 x 1.5 m bin with an accuracy of ±1.0 mm and at a data collection rate of 2 points per second.

The profiler consisted of a laser and a digital camera for height measurements, and a drive system for horizontal movement. The device was calibrated to determine the accuracy of horizontal positioning and the error associated with the height measurements. The positioning accuracy of the profiler was ±0.12 mm and the calibrated height error was ±0.68 mm. The rate of data collection was 32 points per minute.

The calibrated height measurement unit was tested with actual soil samples. The analysis of the data collected from 9 different soil colors at 3 different heights and 5 different locations along the profiler indicated that color, rod deflection, and vertical distance between the lens and the surface affected the height measurements. The error for absolute heights was 1.2 mm and the error for the difference in heights was 0.2 mm.

The outdoor performance of the profiler was also checked and the result was satisfactory.

ACKNOWLEDGEMENTS

The author expresses his deepest appreciation and gratitude to his major professor, Dr. R. K. Byler for his valuable guidance and positive attitude in dealing with the problems during this work. Appreciation is also due Dr. T. A. Dillaha and Dr. J. V. Perumpral for serving on the advisory committee and supporting the author and the study. Author is thankful to Mr. C. F. Adkins and Mr. S. L. Spradlin for their help in building the system. Special thanks is due Mr. P. W. McClellan for his help and patience in the laboratory. And finally, special thanks and gratitude to all those who have given the author the opportunity and the support to come all this way.

TABLE OF CONTENTS

ABSTRACT.....ii

ACKNOWLEDGEMENTS.....iii

LIST OF TABLES.....vii

LIST OF FIGURES.....ix

I. INTRODUCTION.....1

II. OBJECTIVES.....3

III. LITERATURE REVIEW.....4

A. Types of Soil Profile Meters.....4

1. Manual, Contacting Profilers.....4

2. Mechanical, Contacting Profilers.....7

a. Probe type.....7

b. Pin type.....11

3. Mechanical, Non-Contacting Profilers.....13

B. Profile Meter Applications.....15

IV. THE PROFILE METER.....20

A. Design and Construction.....20

1. Profiler Components.....20

a. Digital camera.....26

b. Laser.....29

c. Stepper motor.....33

2. Control Systems.....33

a. Camera control circuitry.....33

b. Motor control circuitry.....37

B. Principle of Operation.....42

C. Control Software.....44
1. Camera Control Software.....44
2. Motor Control Software.....47
3. Height Calculation Software.....48
D. Error Analysis and Calibration.....56
1. Error Analysis.....56
2. Calibration.....59
a. Height measurement calibration.....63
b. Horizontal movement calibration.....64
E. Data Analysis and Discussion.....65
1. Data Analysis.....65
2. Discussion.....72
V. DESIGN OF THE NEW CAMERA.....76
A. Error Analysis.....76
1. Full vs. Half RAM Surface.....76
2. 50 mm vs. 16 mm Lens.....76
3. NOALTBIT vs. ALTBIT Mode.....87
4. Parallel vs. Slanted RAM-Lens Arrangement.....87
B. Construction of the New Camera.....88
C. Calibration and Data Analysis.....89
D. Testing the New Camera with Actual Soil.....92
E. Analysis of the Actual Soil Data.....95

F. Profiler Performance in the Sun Light.....102
G. The New Design Discussion.....102
VI. SUMMARY AND CONCLUSIONS.....107
VII. SUGGESTIONS FOR FURTHER RESEARCH.....110
LITERATURE CITED.....112

APPENDIX A Camera Control Software.....115
APPENDIX B Stepper Motor Control Software.....118
APPENDIX C Height Measurement Software.....122
APPENDIX D Height Measurement Calibration Data Collected by the Camera with the 16 mm Lens.....125
APPENDIX E Horizontal Movement Calibration Data.....130
APPENDIX F Height Measurement Calibration Data Collected by the Camera with the 50 mm Lens.....132
APPENDIX G Calibration Software.....137
APPENDIX H Soil Data.....139
VITA.....140

LIST OF TABLES

1 Optic RAM Dimension.....28

2 Picture Transmission Time (ms) at 9600 Baud Rate and Above.....30

3 Laser Specifications.....31

4 Laser Power Supply Specifications.....32

5 A6 T/D PTM Relative Addresses.....38

6 A6 T/D Base Counter Addresses.....39

7 Command Required for Different Picture Sizes.....46

8 Error Terms at Different Heights for the 16 mm Camera in ALTBIT Mode 60

9 Error Terms at Different Heights for the 16 mm Camera in NOALTBIT Mode.....61

10 E_{rss} and % E_{rss} for the Camera with the 16 mm Lens in ALTBIT and NOALTBIT Modes.....62

11 A Comparison Between Residual Mean Squares (RMS) of Model 1 (Equation (21)), Model 2 (Equation (22)), and Model 3 (Equation (23)) Using the Camera with the 16 mm Lens....67

12 Statistical Results for Horizontal Movement Calibration Obtained from the Data for the First Method.....68

13 Mean and Standard Deviation of the Data Collected by the Second Method for Horizontal Calibration.....69

14 Results of Error Analysis for the Camera with the 16 mm Lens in ALTBIT Mode.....80

15 Results of Error Analysis for the Camera with the 16 mm Lens in NOALTBIT Mode.....81

16 Parameters Used in Error Analysis for the Camera with the 16 mm Lens.....82

17 E_{rss} and % E_{rss} for the Camera with the 16 mm Lens in Two Modes of Operation.....83

18 Results of Error Analysis for the Camera with the 50 mm Lens in ALTBIT Mode.....84

19 Results of Error Analysis for the Camera with the 50 mm Lens in NOALTBIT Mode.....85

20 E_{rss} and % E_{rss} for the Camera with the 50 mm Lens in Two Modes of Operation.....86

21 A Comparison Between Residual Mean Squares (RMS) of Model 1 (Equation (34)) and Model 2 (Equation (35)) Using the Camera with the 50 mm Lens.....93

22 Colors of Soil Samples.....94

23 Results of DMRT Using Model DIF1.....98

24 Means, Standard Deviations and Standard Error of Means for the Data at Levels 1, 2, and 3 Using Model DIF1.....99

25 Results of DMRT Using Model DIF2.....100

26 Means, Standard Deviations, and Standard Error of Means for the Data at L2-L1 and L3-L2 Using Model DIF2.....101

LIST OF FIGURES

1 Schematic of the Soil Profile Meter.....21

2 Camera-Laser Plate: Front View.....22

3 Camera-Laser Plate: Rear View.....23

4 Motor-end of the Profile Meter.....24

5 Gear-end of the Profile Meter.....25

6 The 256 x 256 Optic RAM and the "Honeycomb" Pixel Arrangement.....27

7 Block Diagram of the A6 T/D Board.....34

8 Block Diagram of the R2D23 Board.....35

9 Principle of Height Measurement.....43

10 A 128 x 64 Picture of the Laser Beam as Displayed on the Screen of Apple II.....50

11 Flow Diagram of the Control Software.....57

12 Error vs. Number of Steps at the Motor-end of the Profile Meter.....70

13 Error vs. Number of Steps at the Gear-end of the Profile Meter.....71

14 Residual vs. Measured Height for Equation (22).....73

15 The New Camera and Laser Arrangement.....77

16 Schematic of the New Camera.....90

17 Residual vs. Measured Height for Equation (35).....105

Chapter I

INTRODUCTION

Soil surface height measurements are essential to erosion studies. Soil erosion is an important research subject in agriculture, since it directly affects land productivity and causes water and air pollution. Much research work is being conducted on soil erosion to help researchers better understand the mechanisms of erosion and factors affecting it. The profiles obtained from soils undergoing erosion must be analyzed and compared to describe the erosion phenomenon and to devise new procedures and methods to control erosion. Soil profiles are also important in the evaluation of tillage, seedbed characterization surface water storage and off-road vehicle performance.

A soil profile meter is a device used for making soil surface height measurements. Soil profile meters have evolved from manually operated, contacting machines to mechanically operated non-contacting devices over the past several years. The first set of profile meters were manually operated and contacting devices which used one or more pins for height measurements. Data were recorded manually or photographically.

Since manually lowering the pins to the surface was a slow process, motors were utilized to both automate the lowering task and speed up the data collection. In many cases automation resulted in utilizing a single probe which could be lowered to the soil surface and moved in horizontal direction(s) on controllable grids. Data collection was accomplished manually, photographically, or electronically.

Further development in profile meter design replaced the contacting pins or probes with opto-electronic devices which eliminated the problems caused by soil contact. The height measurements were obtained in a transect or transects on grids of different sizes. In some instances a light source was projected onto the soil surface and the reflection was focused and gathered onto a photo-sensitive surface. The height was then related to either a horizontal displacement on or the voltage output of the photo-sensitive surface.

The mechanical, non-contact soil profile meter enables the researchers to collect a large number of soil profiles with greater precision and speed than the manual, contacting profilers without disturbing the soil. The design and construction of an automatic, non-contact soil profile meter for this thesis project was motivated by a laboratory soil erosion study. The overall objective of the research was to build an accurate and fast profiler with more versatility than other soil profilers.

Chapter II

OBJECTIVES

The objective of the research was to design and construct a mechanical, non-contact soil profile meter to be used in erosion studies under laboratory conditions with the following design constraints:

1. Measure soil profiles on flat and sloped surfaces.
2. Cover a surface area of 1.5 m by 1.5 m.
3. Be precise to within ±1 mm in both horizontal and vertical measurements.
4. Be fast in collecting data (two data points per second) and moving in the horizontal directions.
5. Be portable and versatile.

Chapter III

LITERATURE REVIEW

3.1 TYPES OF SOIL PROFILE METERS

Over the past few decades a considerable amount of design work has been devoted to soil profile meters. Three types of profilers have been developed (a) manual, contacting type; (b) mechanical, contacting type; and (c) mechanical, non-contacting type.

3.1.1 Manual, Contacting Profilers

Early profilers were manually operated and contacting and in most cases used a row of vertical pins for height measurements. Kuipers (1957) constructed a profile meter to measure soil surface roughness for tillage studies. His profiler consisted of an aluminum frame which held a 2 m long 10 cm high vertical scale. The vertical scale was divided into 1 cm intervals, and 20 needles, set 10 cm apart, were placed in front of it by a spring-mounted bar. The profile meter was supported by two pins and was held in position over the soil surface in detachable handgrips. The device was leveled horizontally by an adjusting screw and an air level. And then the 20 needles were lowered onto the soil by pushing the spring-mounted bar. The heights were measured relative to the lower edge of the vertical scale with an accuracy of 0.5 cm and recorded manually.

Van Ouwerkerk, Pot, and Boersma (1982) developed an electronic micro-relief meter for seedbed characterization, similar to the profile meter designed by Kuipers (1957). The micro-relief meter consisted of ten 383 mm-long plexiglass measuring rods, 10 opti-couplers, a lifting bar, and a 270 x 274 x 100 mm steel frame. The rods passed through the

slots, set 2.5 cm apart on the lifting bar, and had 200 blackened grooves. The data were collected in 2.5 cm grids over 270 mm transects by lowering the lift bar manually to its lowest level (183 mm above the steel frame) and allowing the rods to touch the surface of soil in the steel frame. As the rods passed through opti-couplers, the number of grooves were counted by binary-coded decimal (BCD) counters, converted to their equivalent ASCII codes, and recorded on a cassette recorder. Each reading (10 per transect) took about 5 seconds. Transfer of data into punch cards, calculation of seedbed depth and roughness of 700 readings, and drawing of the cross section using a computer took about 15 minutes.

Curtis and Cole (1972) developed a micro-topographic profile gage similar to that of Kuipers to study erosion on surface-mined lands. This device consisted of a row of 40 vertical pins spaced 30 mm apart and a backboard with horizontal lines forming grids with the pins. In order to measure the soil surface heights, the gage was placed on reference stakes, the pins were lowered to the ground surface forming the profile of the soil on the backboard, and a picture was taken from the board. The films were analyzed and compared to find the soil loss or deposition from the difference in height at each point at different dates.

Dexter (1977) built a soil profiler to conduct a study on tillage. This profiler was comprised of a 300 cm long frame with a needle for elevation measurements. The needle could move horizontally across the frame with 600 positions for elevation measurements. The profiler could measure heights ranging from 1 to 50 cm with an accuracy of 0.1

cm. The time required for two people to read 500 elevations on a transect was 40 minutes.

Wilton (1964) constructed a soil profiler to investigate the effect of different cultivations on crop yield and also to detect the vertical movement of soil surface under barley and sugar beet crops. The profiler consisted of two steel stakes buried in the soil over which two drain tiles were placed. A box-like aluminum beam was placed over the two stakes by two pointed legs 2.7 m apart. Several aluminum rods were fitted into 2.5 cm spaced holes over the center 1.5 m length of the beam for height measurements. The pins passed through a bar which held them above the soil surface. The height measurements were made by lowering the bar and letting the rods rest on soil surface and recording the distance each rod moved vertically. It took two people 3 min. to set up the profiler and collect the data over one transect.

Riley (1983) constructed a soil profiler to measure soil surface changes for erosion studies. His profiler consisted of a contouring frame, a measurement bar with a sliding vernier attached to it, and two supporting frame bars. The two supporting bars and the measurement bar were made of 1.2 m long square steel bars. There were eleven holes spaced in intervals of 10 cm along the frame bars. A total of 100 heights were measured over a 1 m x 1 m plot. The vernier was accurate to 0.1 mm but the actual vertical accuracy of the device was 2 mm with a horizontal variation within a circle of 1 cm radius.

In addition to being slow, the manual and contacting profilers were inaccurate due to penetration of pins into soft soil, rupture and deformation of soil clods by the pins, and accumulation of mud on the tip of

the pins from contact with wet soil. Because the data collection was performed manually, human errors were also inevitable. These profilers, once constructed, did not offer the flexibility in having different grid sizes which limited their applications and affected their accuracy. Since they were designed to measure heights of only one transect at a time, it was necessary to replace, relevel, and readjust the profiler every time at every new transect. The above problems which affected the speed and accuracy of the manually operated profilers led to development of mechanical profilers.

3.1.2 Mechanical, Contacting Profilers

The next generation of soil profilers consisted of mechanically operated and contacting profilers which either used vertical pins or a probe for height measurements. The horizontal and vertical movements of pins and probe were accomplished by motors.

3.1.2.1 Probe type

Heermann, Wenstrom, and Evans (1969) constructed a semi-automatic soil profiler to measure soil surface roughness for prediction of flow resistance in furrows. The profiler consisted of a 14.6 m long, four-section, portable truss with adjustable rails for carrying the height measuring unit. The truss was set in parallel with the bottom of the 61 m long soil test channel. A probe, using a potentiometer, was used to measure soil roughness profiles. One motor moved the probe in the vertical direction and a second one moved the measuring unit forward. Two 12-V batteries supplied the power to the motors. The roughness measurements were made in increments of 0.32 cm over a 2.0 m distance after each water run.

Schafer and Lovely (1967) developed a mechanical profile meter to study the effect of tillage on soil surface. Their profile meter consisted of a probe mounted on a carriage, a horizontal frame, and an aluminum tripod. A motor moved the carriage in the horizontal direction through a rack and pinion. Another motor moved the probe vertically for height measurements. The meter was supported by an aluminum tripod which also provided leveling. The profiler collected data every 25 mm over a 2.1 m distance. The heights were recorded on a strip chart for later studies.

Currence and Lovely (1971) added another dimension to the profile meter developed by Schafer and Lovely. It consisted of a main frame in addition to the crossframe, probe carrier, and the probe of the previous device. Three bubble levels and four adjustable legs facilitated the leveling of the profile meter. The main and crossframes were constructed of aluminum channel. A synchronous motor drove the crossframe 1.5 m over the mainframe with a rack and pinion. The probe carrier was also made of aluminum and mounted on the crossframe. Another synchronous motor drove the probe carrier 2 m horizontally through rack and pinion along the crossframe. A third motor, moving the probe vertically, was mounted on the carrier. The locations of crossframe and probe carrier (x and y coordinates of each point) were determined by actuating snap action switches located at 2.5 cm increments along the racks. The height measured (in form of mechanical probe travel) was converted into analog voltage signal by a ten-turn potentiometer geared to the probe. The analog signals were converted to digital for computer use. The height of each point and its x-y coordinates were recorded on punch

cards. 4800 height readings were taken over an area of 1.5 m by 2.0 m on a 2.5 cm grid with an accuracy of ±1.27 mm in 3 to 4 hrs.

Mitchell and Jones (1973) developed a profile measuring device (PMD) to quantify micro-relief surface depression storage and its effect on the rainfall-runoff phenomenon. This device was similar to that of Currence and Lovely except that it was more compact and used more advanced components. The PMD consisted of a probe, a probe carriage, a cross frame, a main frame, a power supply control unit, and a recording unit. The main frame was constructed from aluminum and consisted of a synchronous motor, sprockets and chain to move the cross frame 89 cm horizontally and four adjustable legs. The cross frame consisted of a synchronous motor with chain and sprockets to move the probe carriage and the snap-action switches to signal the position of the probe. The probe carriage contained the probe, a synchronous motor to move the probe, snap-action switches, and a potentiometer and its power supply. The height measurements corresponding to the vertical travel of the probe were measured by the potentiometer as proportionate voltages. The data were collected on 2.5 cm grids and recorded on punch cards. A total of 1225 height measurements could be recorded in 1 $\frac{1}{2}$ hrs. Replacement of the snap-action switches was required after 210,000 measurements.

Henry, Sciarini, and Van Doren (1980) developed a soil profiler to measure soil profiles and soil surface roughness for agronomic studies. This device consisted of a main frame, a probe carriage, and a probe. The main frame had adjustable legs and level bubbles for vertical distance adjustment and leveling. The probe carriage was moved

along the main frame by a 6 VDC gear motor, a miniature cog belt, and a bicycle chain. The probe could move vertically by a 12 VDC motor, a cog belt, and a gearhead. The probe consisted of a ten-turn potentiometer for vertical travel measurement of the probe, a sensor wire for signaling the contact of probe with the soil, and a Hall-effect switch with reversing circuitry for reversing the motor and sending the probe up and away from the soil surface. The soil surface heights were printed out as proportional voltages after the probe was lowered and touched the surface. A Hall-effect switch was used to advance the probe carriage 2 cm after each measurement along the 2 m long cross frame. After completion of each transect (100 data measurements) the probe was raised and brought back to the starting position with a speed of 76 to 165 cm per min. It was possible to collect 100 data points in 1.2 to 2.7 min over a 2 m distance at 2 cm grids.

Podmore and Huggins (1981) constructed a profile meter to measure sand profiles for a study of overland flow influenced by surface roughness. Their device consisted of a cross carriage which travelled on linear bearings on a steel shaft placed on an aluminum back bone. A linear variable differential transformer (LVDT) with an extension range of ±13 mm was used for the height measurements. The LVDT core was bonded to a surface elevation sensing probe and a phonograph needle was fastened to the lower end of the probe shaft tip for ease of data collection in 0.25 mm intervals. The carriage drive system contained a bi-directional stepper motor, rack and gear and was mounted on the carriage.

Before data collection, the profile meter was positioned and leveled on the flow surface bed and the height, was adjusted. Then the probe was lowered to surface and the height measured by LVDT in form of voltage output, was trasmitted to an analog/digital hybrid computer and recorded on magnetic tape. The profile meter measured 7400 heights over a length of 1.85 m at 0.25 mm intervals in 2 hrs. The data were accurate to within ±0.005 mm over a 33 mm range. The main problems with this profiler were deflection of the probe tip and penetration of the needle into soft soil due to high pressure created on its contact area by the mass of the sensing unit.

3.1.2.2 Pin Type

Radke et al. (1981) constructed a rillmeter to study the erosion and rill development caused by rainfall. The profiler consisted of an aluminum frame and a movable platform holding 312, 45 cm long, pins. The pins were arranged in 3 rows, 5 cm apart, and 104 columns, 1 cm apart. A 12 VDC gear motor with chain and sprockets was used to raise and lower the platform.

In order to collect the surface height readings, the rillmeter was positioned over the soil surface and the platform was lowered until all the pins touched the surface of soil. As a pin struck the surface a spring switch opened and the microprocessor scanning the switches recorded the height of that point. An optical switch and a disk with 2 holes were used to indicate the vertical position of the platform and the heights of the points. The data were stored on cassette tape. The data (312 points) were collected with an accuracy of 1 mm over a verti-

cal distance of 25 cm in 1 min. The drawback of this device was unreliability of the sensing switches.

Hirschi, Barfield, and Moore (1984) designed two mechanical and contacting pin-type soil profilers for use in erosion studies. One profiler was 4.5 m long with 70 pins spaced in 6.4 cm intervals, and the second one was 1 m long with 72 pins set in 1.3 cm intervals. A movable frame was mounted in front of each profiler. The frame movement was achieved by 110 VDC solenoids and return springs were used to facilitate the free fall of the pins. A level bar, riding in guides, lowered the pins until all of them rested on the soil, the pin displacements were measured by a voltmeter and recorded on magnetic disk, the pins were raised, and unit moved to next position for more data collection. Lowering of the pins was accomplished by a reversible gearmotor through remote control.

The electronics of the profiler consisted of a pin displacement circuit, a computer control circuit, and a bar movement control circuit. The pin displacement circuit was basically a voltage-divider driven by a 12 VDC power supply. The computer control circuit comprised of two parts. The first was a 3 VDC circuit through which operator could signal the computer to prepare the profiler and take data, process or retake data, and stop the data collection. The second part was a 12 VDC circuit used by the computer to respond back to the operator. The bar movement control circuit used a switching circuit to control the reversible gearmotor.

The height measurements were obtained by a data acquisition unit and a microcomputer with an interface board. Field plots of 22 m x 4.5

m area and slopes up to 30 percent were studied and the height measurements with ±1 mm accuracy were recorded from single transects in less than 1 min.

Although automation of contacting profilers improved the speed of data collection and reduced human errors, the problems caused by contact of pin and probe with the soil surface still existed. The pin-type profilers improved the speed of data collection, but did not offer the grid size flexibility as the probe-type did. The accuracy of height measurement was affected by inflexible grid sizes and the problems due to contact (e.g., deformation of soil surface, penetration of pin/probe into soil and diameter of contact mechanism). The problems resulted from contact with soil along with the great effort put into construction of the pins and the probe, complexity of the control systems, and bulkiness and weight of contacting profilers (especially the pin-type) led researchers to design of mechanical, non-contact profilers.

3.1.3 Mechanical, Non-Contacting Profilers

The third and the most technologically advanced type of profilers were mechanically operated and non-contacting which often used optical devices for height measurements.

Romkens, Singarayar, and Gantzer (1982) developed a mechanical, non-contact surface profile meter to measure soil surface profiles in the study of the effects of rainfall on tilled soils. The meter consisted of a probe, a probe carriage, and the main frame. The probe and the vertical drive system were mounted on the carriage. The carriage was placed on two parallel steel rods with 4 ball bushings. The horizontal movement of the carriage and the probe was accomplished

by a 12 VDC motor through a ball bearing screw. The vertical movement of probe was made possible by a moveable ball bearing screw and a servo motor. The horizontal and vertical positions of the probe were monitored by encoders attached to ball bearing screws. The probe was made of an infrared light emitting diode (LED) and a phototransistor which moved at a 10 to 15 mm distance parallel to the soil surface.

The data were collected in transects of 1.52 m long by positioning the profiler on an aluminum base over the experimental soil surface. The vertical and horizontal coordinates of artificially colored and shaped surfaces and real soils were collected with the profiler and a point gauge and recorded on a magnetic tape. Up to 250 points per meter were collected in every transect with an accuracy of ±2 mm in 4 minutes.

Harral and Cove (1982) developed an optical displacement transducer to study the seeding depth control on cereal drills by measuring the soil surface profiles. The transducer was composed of a laser diode, a lens in a 15-degree angle with the diode, and a photodetector mounted on a printed board.

The principle of operation was based on collecting the reflected light from the soil surface and focusing it on the detector surface. The reflected light moved on the surface of the detector, as the soil height changed, and an output voltage proportional to the reflected light position was recorded.

The device was calibrated for static and dynamic performances by performing a number of tests on several materials resembling different soils. The accuracy of this device was affected by noise in the output,

size of the laser beam, and reflectivity of soil surface. The overall error was ±6 mm for a range of ±15 mm, 600 mm above the soil surface.

Contactless and mechanical profilers solved many problems associated with the contacting type profilers. They simplified the construction by replacing the probe and the pins and, in some cases, their vertical movement control system with an opto-electronic device. Moreover missing data due to inadequate light reflecting from the surface, sharp angles of soil clods, or light reflected from the surface being out of the range of light-sensitive detector was a common problem in the contactless type profiler. Interpolation has been used (Harral and Cove, 1982) to replace the missing data.

3.2 PROFILE METER APPLICATIONS

Different soil profilers have been in use during the last few decades. The studies have been directed at tillage assessment, off-road vehicle dynamics, micro-relief surface storage, seedbed preparation, and others.

Kuipers and Van Ouwerkerk (1963) used the soil profiler constructed by Kuipers (1957) to estimate total porosity of freshly plowed soil from the pore space of the unplowed soil from soil surface height measurements.

Burwell, Allmaras, and Amemiya (1963) used a manually operated, contacting soil profiler to collect elevations of a plowed layer of soil to study the effect of tillage on the porosity of the layer. Soil elevations were measured on 5 cm by 5 cm grids over an area of 1 sq m

with an accuracy of 2.5 mm. Measurements were made before and after tillage.

Currence and Lovely (1970) used their profiler to measure soil surface roughnesses for a tillage study. Their aim was to correlate soil surface roughness with soil properties (e.g., soil temperature, moisture content, etc.) affecting tillage and, therefore, crop production for possible elimination of their measurements. Their study included description of surface roughness of several tilled soils by roughness indices, utilization of power spectral density analysis in finding surface irregularities, and determination of the number of height readings necessary for estimation of the roughness index.

Merva et al. (1970) used a soil profiler for watershed surface description. Height readings of two sloped surfaces were obtained in 2 cm intervals over 3 meter distances for their study. They investigated the difference between micro- and macro-surfaces and used the micro-surface measurements for overland flow analysis.

Dexter (1977) used his profiler to measure "the surface micro-reliefs after four different tillage treatments" to study the "effect of rainfall on the surface micro-relief of tilled soil." "The relief measurements were used to calculate the auto-correlation functions, the power spectra, and the distributions of surface slopes." He concluded that roughness indices provided more information about the change in relief with raindrop impact than did autocorrelation function and power spectrum.

Mitchell and Jones (1976) used a profiler to conduct a study on the "micro-relief surface depression storage." The height measurements were

made from five different soil surface areas of 90 cm by 90 cm and three artificial surfaces with an accuracy of ±1.27 mm. The data were analyzed to develop models for describing the surface depression storage. The data analysis was carried out by using five storage-computing methods, 15 different depth-storage models, and 3 grid sizes.

Mitchell and Jones (1978) used the same profiler to conduct another study on micro-relief surface depression storage. Micro-reliefs of 88 soil samples from 4 different soil types were measured before and after artificial rainfalls with various intensities and durations. The data were analyzed to develop models which could describe the change in micro-relief surface depression storage during a rainfall event. The models which were developed related the changes with rainfall, surface hydrology, and soil parameters as well as their cross products and micro-relief parameters.

Moore and Larson (1979) used a soil profiler to estimate micro-relief surface storage from soil height measurements. The height measurements were taken from a 102 cm by 102 cm plot on a 5 cm by 5 cm grid with an accuracy of 1.25 mm using a soil profiler. The data were collected photographically from both unplowed and plowed soils before and after simulated rainfall. The data were analyzed and a model for estimating micro-relief storage and runoff was developed.

Romkens and Wang (1985) used the noncontact profiler constructed and improved by Romkens, Singarayar, and Gantzer (1982, 1985) to study the soil roughness changes of three different tillage systems caused by artificially simulated rain storms. The roughness measurements were made from a 1.52 m by 1.83 m plot of soil before tillage and after a

rain storm. The study resulted in expressing the soil surface roughness as an exponentially decaying dimensionless parameter, R, which "reflected the effect of clod size and clod frequency per unit transect length." Their study also showed a variation of autocorrelation functions among tillage sytems and within a tillage system following the application of successive rainstorms.

Henry, Sciarini, and Van Doren (1980) used their profiler to estimate "the relative smoothness of different seedbeds." Their studies concentrated on seedbed preparation for planting sugar beets and transplanting tomatoes.

Johnson and Smith (1983) studied the effects of off-road vehicles on soil loss in steep slopes. They employed two different methods for data collection in their studies. The first method used aerial photographs of two different dates and the second method used a rillmeter. The results obtained from the data collected by the rillmeter showed an erodability of about 7 times greater in the upper sections of slopes than the lower sections.

Molnau, Yen, and Druffel (1984) studied the effects of freeze-thaw on surface roughness changes of slopes using the roughness data collected by a microrelief meter. Height reading data were obtained on 12 by 50 mm grid from four test plots of 1 m by 1 m surface area with slopes of 5 to 7% and treated with four tillage systems. Random roughness was computed from height readings. The conclusions drawn from the measurements and tests over a seven-month period showed that the plow with highest initial roughness decreased faster than other plows but had a greater final roughness.

Rogowski, Khanbilvardi, and Jones (1984) conducted an erosion study to compare the amounts of eroded or deposited soil at a point measured by erosion pins with gross measured amounts of erosion and erosion and deposition amounts predicted by mathematical models. Two rainfall simulator plots of 6.5 percent slope and 3 x 9 meter length were used for the study. Forty 1 m long pins were placed on each plot, in 10 rows of 4, to a depth of 90 to 95 cm to be used as fixed reference points for soil erosion or deposition measurements. A washer was slid over each pin and a micrometer was used to read elevation changes after each simulated rainfall. The study of rill development was performed by measuring the cross-sectional changes of soil before and after each rainfall. Eighteen "anchor rods" driven into the soil in 9 rows of 2, 9 horizontal bars attached to each pair of rods, and a metal ruler facilitated the height measurements. The results obtained from pin measurements showed a higher erosion compared with the results from mathematical models. The reason for such difference was explained as the turbulence in flow caused by the pins.

Chapter IV

THE PROFILE METER

4.1 DESIGN AND CONSTRUCTION

A schematic of the profiler is shown in Figure 1. The profiler which was designed and constructed was an automatic, non-contact profiler which consisted of a laser and a digital camera. The camera and the laser were mounted on a 25.4 x 38.1 x 0.6 cm aluminum plate with aluminum clamps. The aluminum plate was held in a vertical position, centered between two parallel stainless steel rods (182 cm long, 1.9 cm in diameter), by two linear ball bearings (Winfred M. Berg, Inc.). The two supporting rods were clamped 21 cm apart to two 12.7 x 24.4 x 0.6 cm horizontal aluminum plates. The horizontal movement of the camera-laser plate (CLP) was accomplished by a stepper motor through a plastic-coated steel chain and two stainless steel sprockets (1.27 cm in diameter). The motor was fastened to one of the horizontal plates and an idler sprocket to another. Figures 2, 3, 4 and 5 illustrate the CLP, the motor end, and the gear end of the profiler.

4.1.1 Profiler Components

The profiler consisted of the height measurement unit, the horizontal translation unit, the control unit, and the processing unit. The height measurement unit was comprised of a laser as the light source and a digital camera as the light sensor. The horizontal movement unit consisted of a stepper motor, a chain and two sprockets along with two supporting rods and two linear ball bearings. The control unit contained several electronics boards which controlled the operation of the

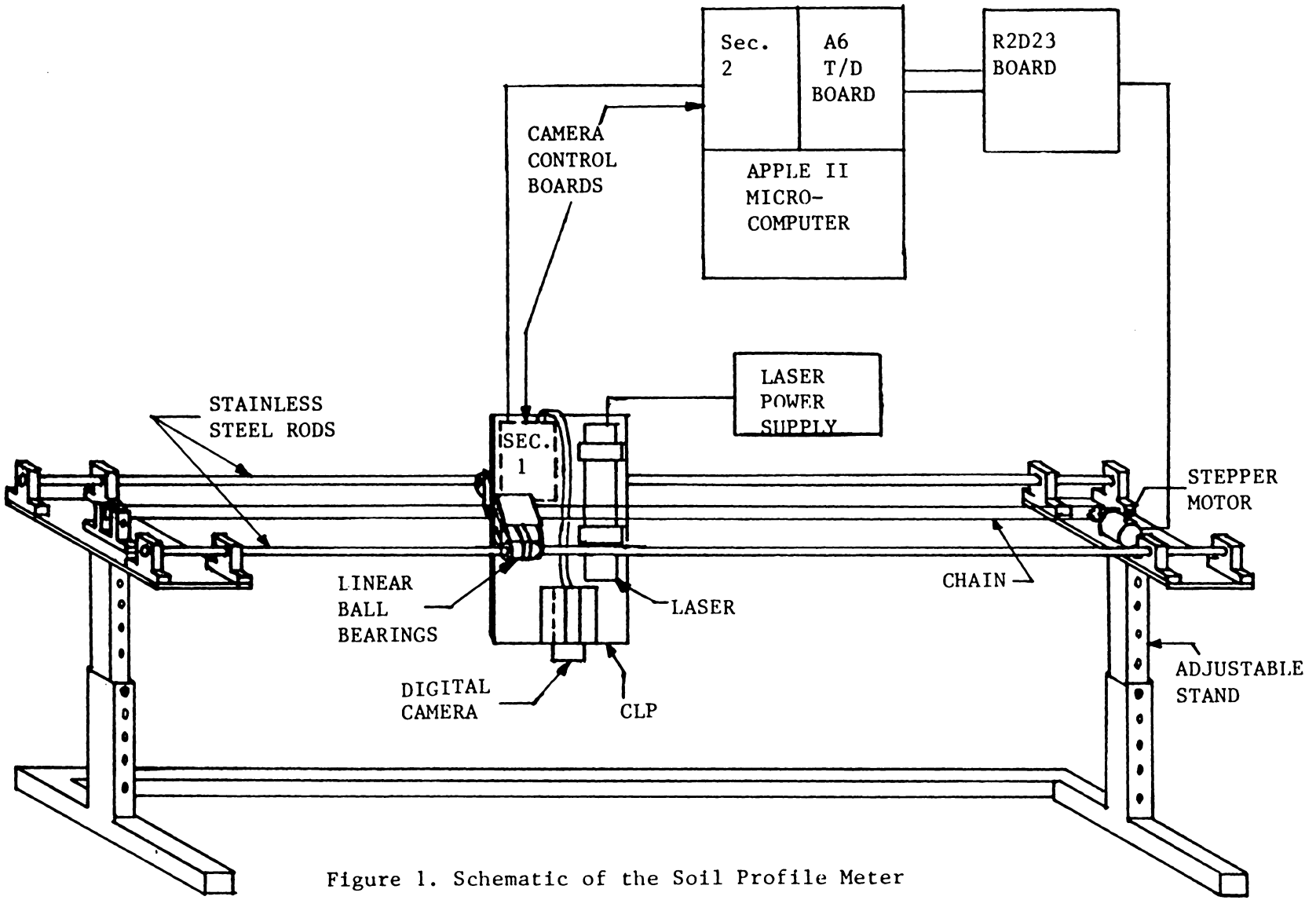

Figure 1. Schematic of the Soil Profile Meter

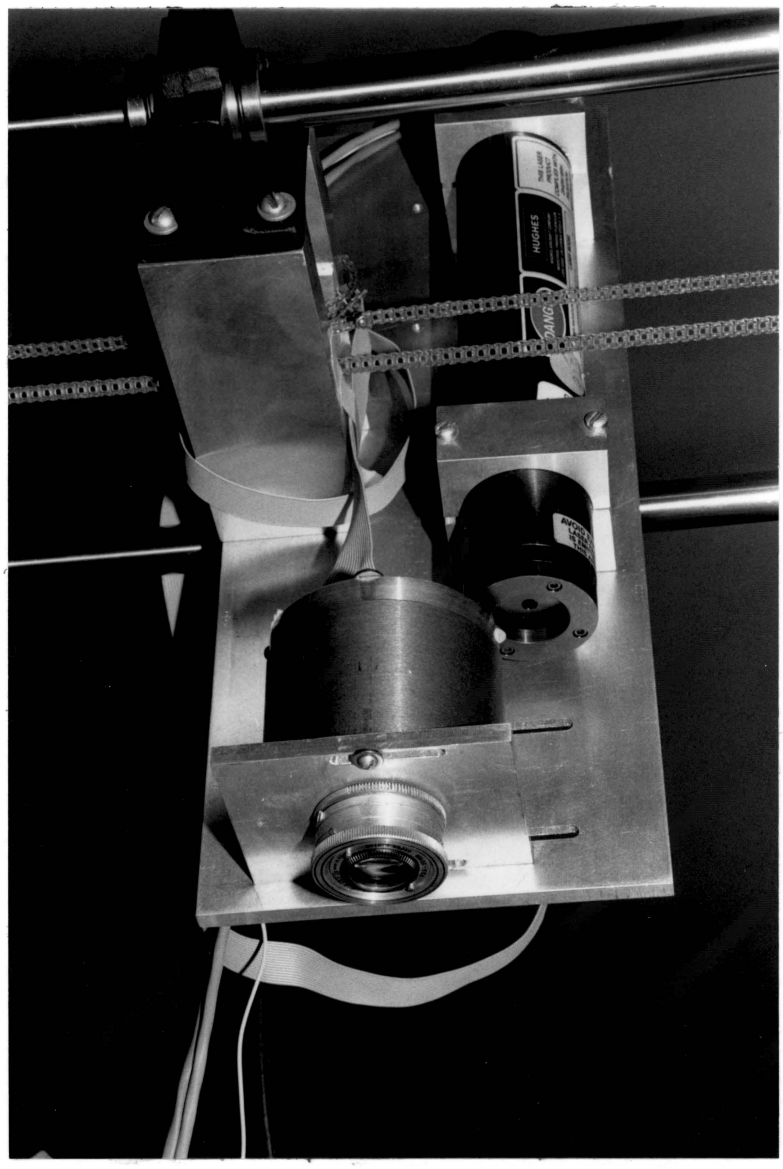

Figure 2. Camera-Laser Plate: Front View

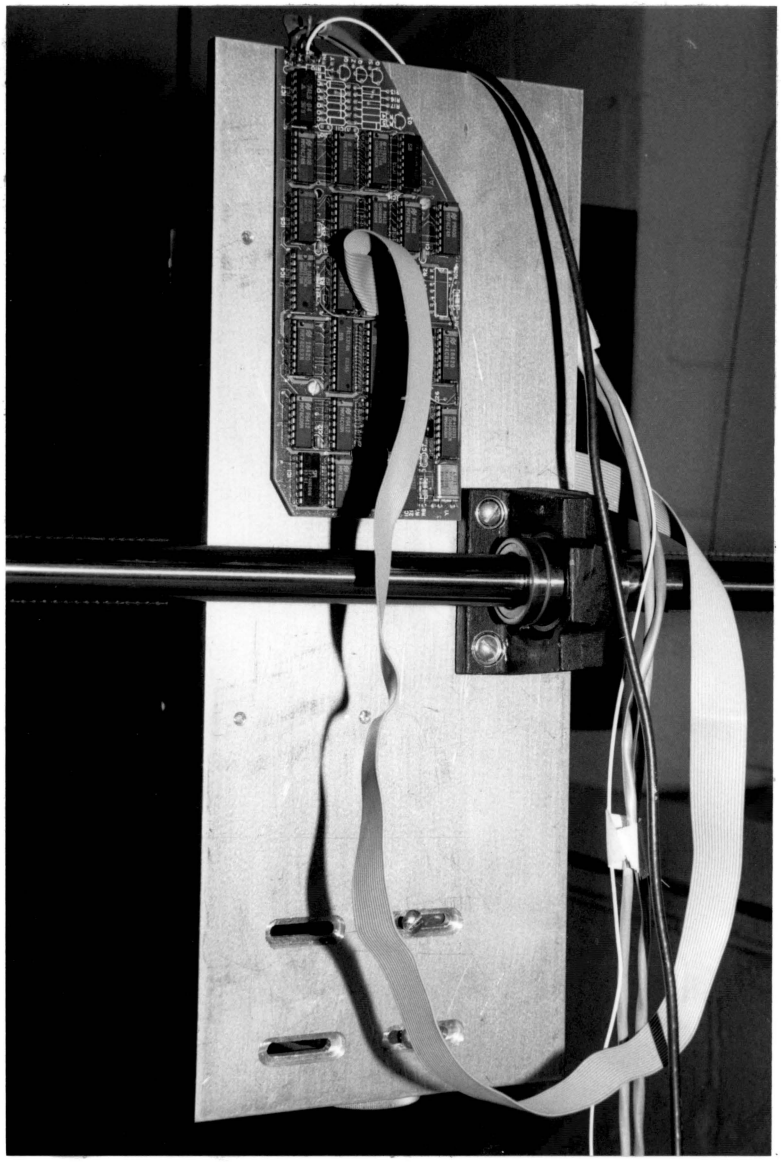

Figure 3. Camera-Laser Plate: Rear View

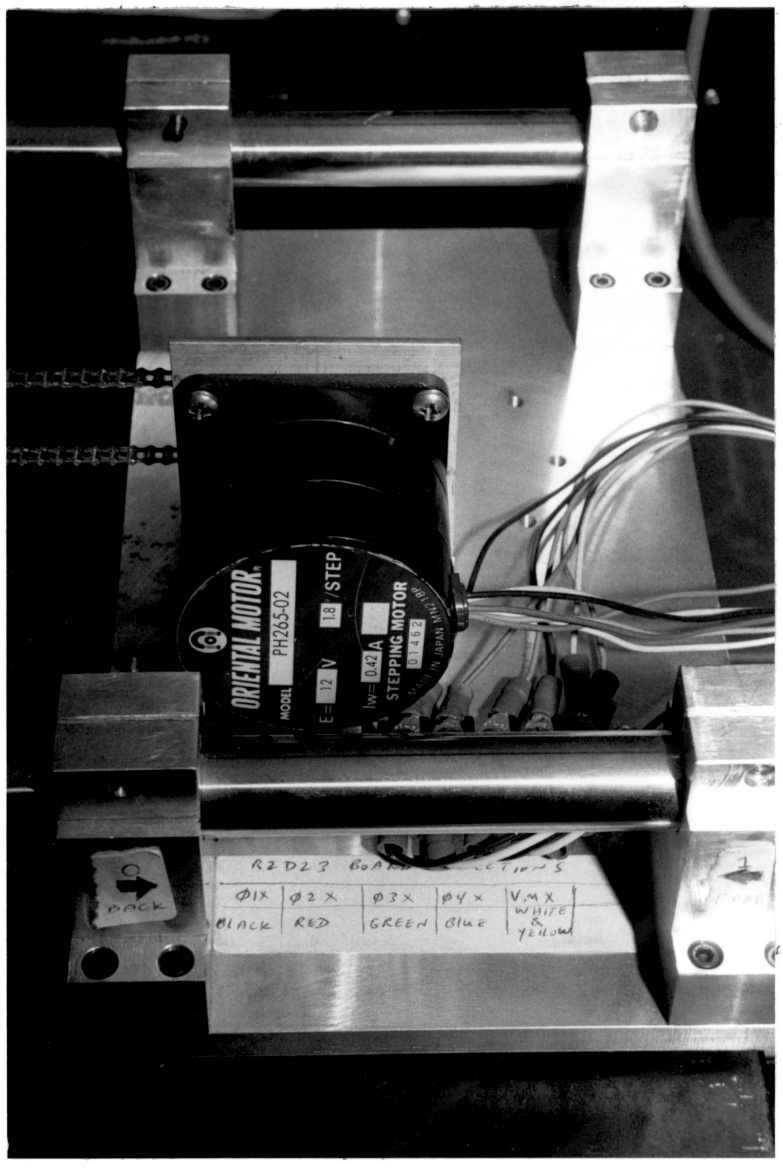

Figure 4. Motor-end of the Profile Meter

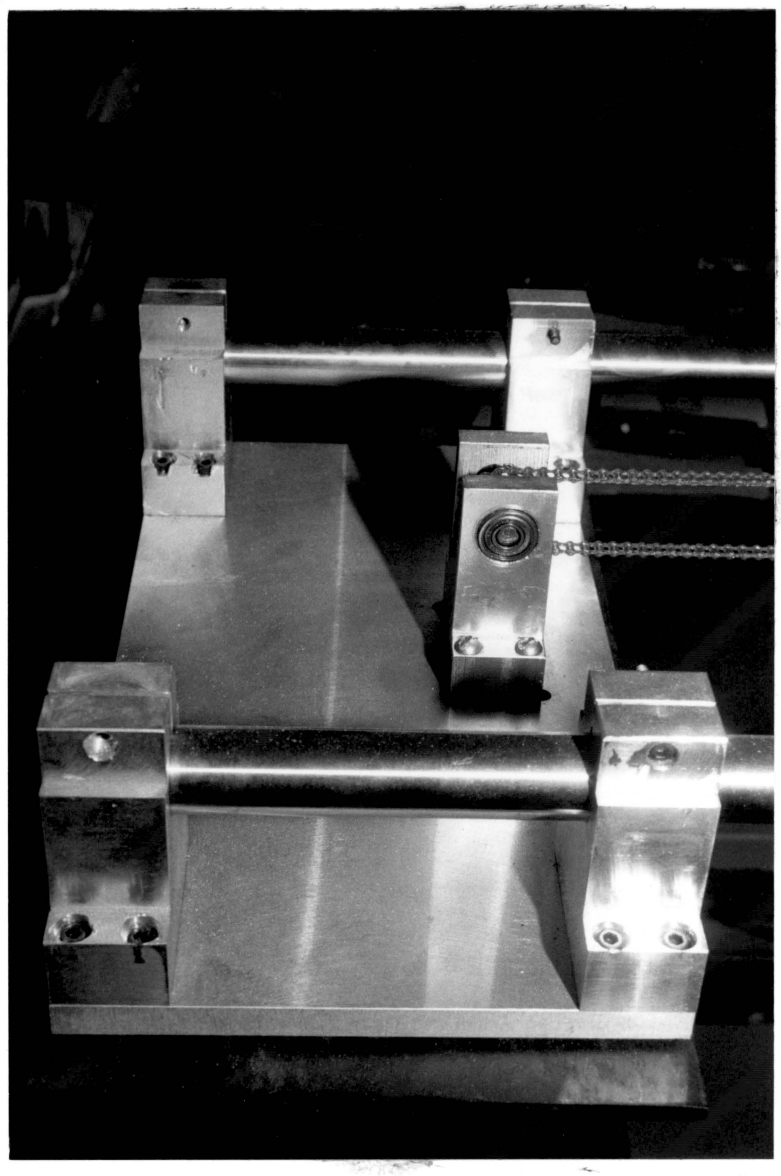

Figure 5. Gear-end of the Profile Meter

camera, motor and laser and interfaced the computer with the camera and motor. The processing unit was a microcomputer with the software developed for height measurement, motor control, and operation of the camera.

4.1.1.1 Digital Camera

The camera (Micromint, Inc., 1983) consisted of a 16 mm C-mount lens and an Optic random access read/write memory (RAM). The Optic RAM was made up of two 128 x 256 arrays of picture elements (pixels). The arrays were separated from each other by a "dead zone." The pixels (light-sensitive capacitors) were arranged in a "honeycomb" configuration, where alternate capacitors from even rows from one array were used, as shown in Figure 6. The arrays were exposed to light through a glass lid. The array dimensions are displayed in Table 1.

The camera operation resembled that of a black-and-white film (Ciarcia, 1983). The RAM pixels were similar to the light-sensitive elements of the film and their binary response to the light. The camera aperture (size of opening, measured in F-stops, which passed the light to RAM surface) was controlled mechanically. The exposure time (shutter speed) was controlled electronically through software by a "SOAK" command which "opened" the shutter and kept it open for the specified exposure. The "REFRESH" command "closed" the shutter and prepared the camera for another picture which was similar to advancing the film.

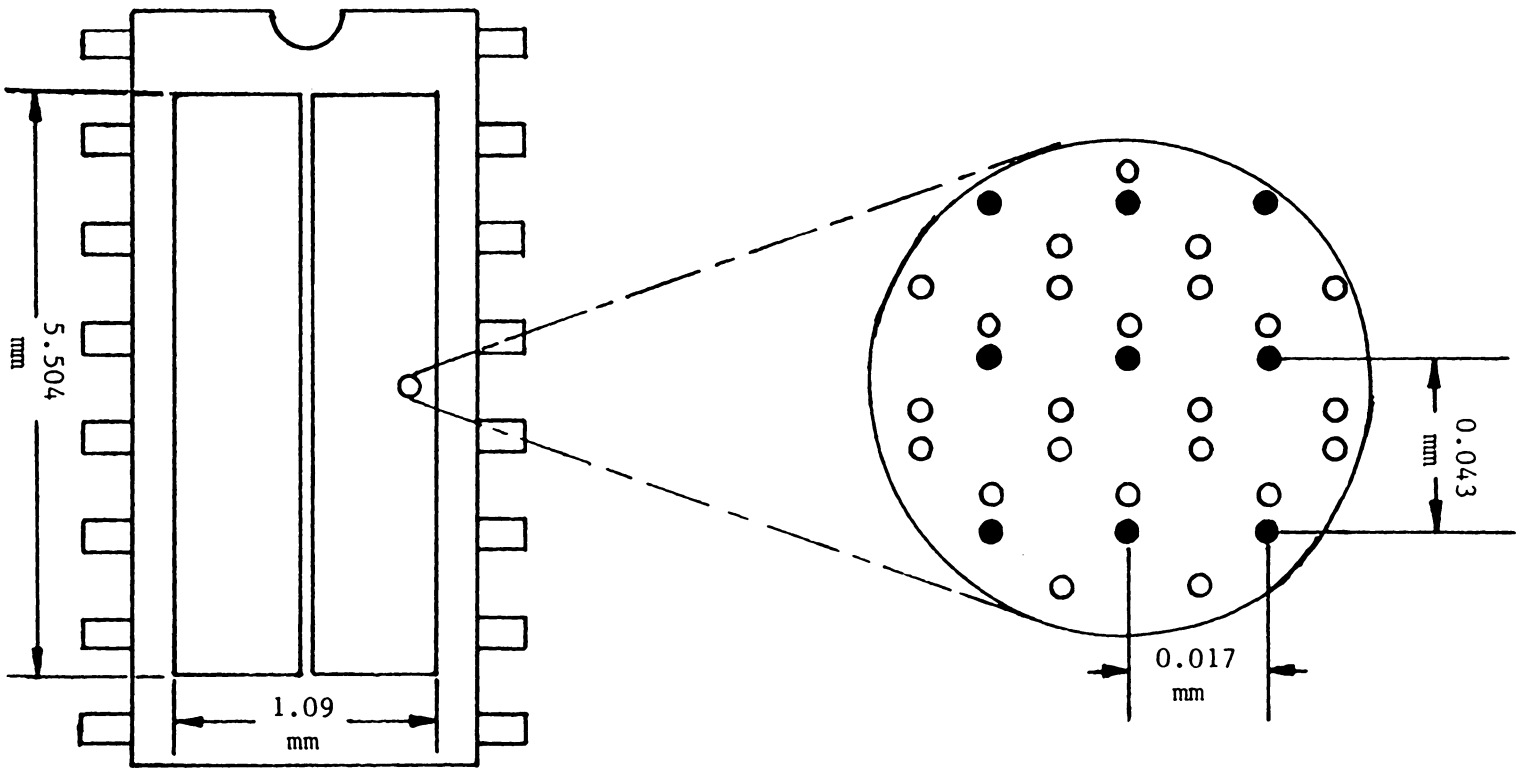

Figure 6. The 256 x 256 Optic RAM and the "Honeycomb" Pixel Arrangement

TABLE 1

Optic RAM Dimension

ELEMENT	DIMENSION (mm)
128 x 256 ARRAY	5.504 x 1.088
PIXEL	0.008 x 0.009
HORIZONTAL SPACING	0.0085
VERTICAL SPACING (CENTER TO CENTER)	0.0215
ALTERNATE PIXELS	0.043
DEAD ZONE SPACING	0.15

A digital picture was formed on the RAM surface. The capacitors, initially charged up to 5 volts, began to discharge when exposed to photons of light. The rate of discharge depended on the light intensity. The light reflected from a surface into the RAM with adequate intensity and exposure time discharged the capacitors through a threshold voltage of +2.1 volts indicating a white surface (logic Ø), while a dim light did not, indicating a black surface (logic 1). The capacitors were accessed by the microcomputer (Apple II Plus) as memory cells. The picture data was transferred from the camera to the microcomputer for display and manipulation at a baud rate of 9600 bits per second (bps).

The time (ms) required to transfer a picture of different dimensions with a baud rate of 9600 and above is shown in Table 2 (Micromint, Inc., p. 27) using Equation (1).

$$\text{TIME} = (\text{Rows} \times \text{Bytes-per-row} \times 10000)/\text{Baud rate} \qquad (1)$$

4.1.1.2 Laser

The laser was a cylindrical helium-neon laser (27.55 cm long, 4.42 cm in diameter) which was operated at 632.8 nm wavelength and had a continuous, polarized power output of 2 milliwatts (Ealing Corp., 1984). The beam diameter was 0.63 mm and had a divergence of 1.3 mrad, which remained uniform over the desirable range of operation. A power supply of 1730 to 2450 VDC energized the laser.

The laser was chosen over other light sources because of its high intensity, small and uniform beam, low power output, and high reliability in operation. Tables 3 and 4 display laser and power supply specifications.

TABLE 2

Picture Transmission Time (ms) at 9600 Baud Rate and Above

ROWS	BYTES PER ROW	BAUD RATE 9600	19200	76800	153600
64	16	1067	533	133	67
64	19	1267	633	158	79
64	32	2133	1067	267	133
64	37	2467	1233	308	154
128	16	2133	1067	267	133
128	19	2533	1267	317	158
128	32	4255	2133	533	267
128	37	4933	2467	617	308
128	64	8533	4267	1067	533
128	73	9733	4867	1217	608
256	32	8533	4267	1067	533
256	37	9867	4933	1233	617
256	64	17066	8533	2133	1066
256	73	19466	9733	2433	1217

TABLE 3

Laser Specifications

OUTPUT POWER	2 mW
BEAM DIAMETER	0.63 mm
BEAM DIVERGENCE	1.3 mrad
POLARIZATION	>500:1
OPERATING VOLTAGE	1780 VDC
OPTIMUM CURRENT	6.5 mA
AMPLITUDE NOISE (RMS)	<1%
LENGTH	275.5 mm
DIAMETER	44.2 mm

TABLE 4

Laser Power Supply Specifications

OUTPUT VOLTAGE	1730 to 2450 VDC
OUTPUT START VOLTAGE	>10 kV
OUTPUT CURRENT	6.5 mA
CURRENT REGULATION	±0.1 mA
BEAM AMPLITUDE	<0.2% RMS
INPUT VOLTAGE	110 VAC
WEIGHT	1.1 kg (2.3 lbs)

4.1.1.3 Stepper Motor

The stepper motor was a single shaft, uni-polar motor with a 1.8 degree step angle and 41.2 N-cm (58.3 oz-in) holding torque (Rogers Labs, Inc., 1984). The motor weighed 0.54 kg (1.2 lbs) and had a rotor inertia of 110 g-cm^2 (0.6 oz-in^2). A timer-driver logic board (A6 T/D) was used to interface the motor with the microcomputer. Another board (R2D23) was used to transmit the power to the motor (12 v) and the logic board (5 v). Figures 3, 7, and 8 show the motor, A6 T/D, and R2D23 boards, respectively. A detailed diagram of the R2D23 and the A6 T/D boards are found in Figures 3-6 and 5-1 of the A6 T/D User's Manual (Rogers Labs, Inc., 1984).

4.1.2 Control Systems

The control unit consisted of the camera and motor operation control systems. A prefabricated board interfaced the camera with the computer. It prepared the camera for operation, received the picture, and transferred it to the computer. A board provided the link between the motor and the computer. Another board supplied the motor with power and provided access to a motor shaft encoder.

4.1.2.1 Camera Control Circuitry

A prefabricated control board was used to interface the camera with the microcomputer (Micromint, Inc., 1983). The board consisted of two sections which communicated through five lines; transmit, receive, external clock, power (V_{cc}), and ground. The first section controlled the camera operation and received the data for the picture. It con-

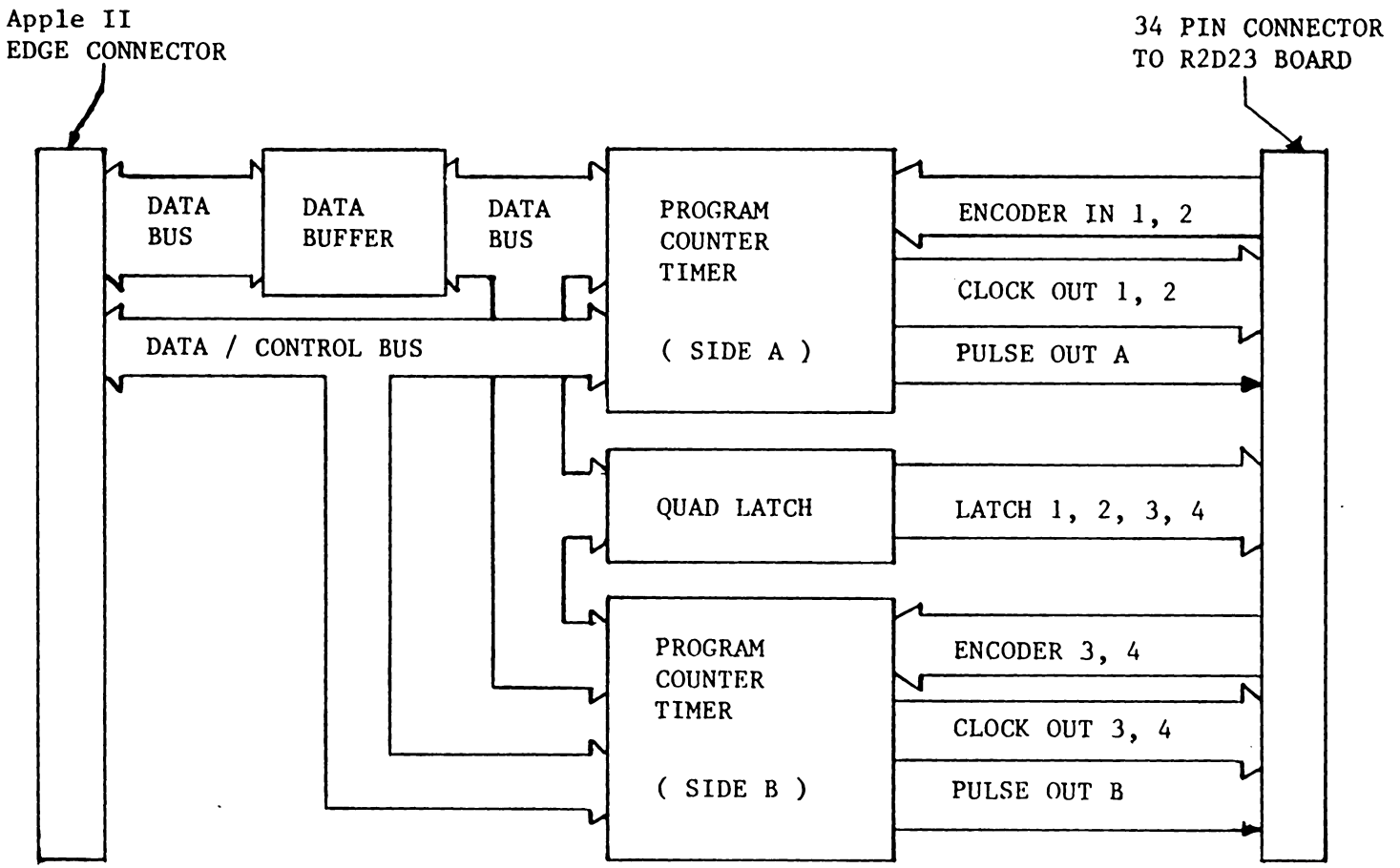

Figure 7. Block Diagram of the A6 T/D Board

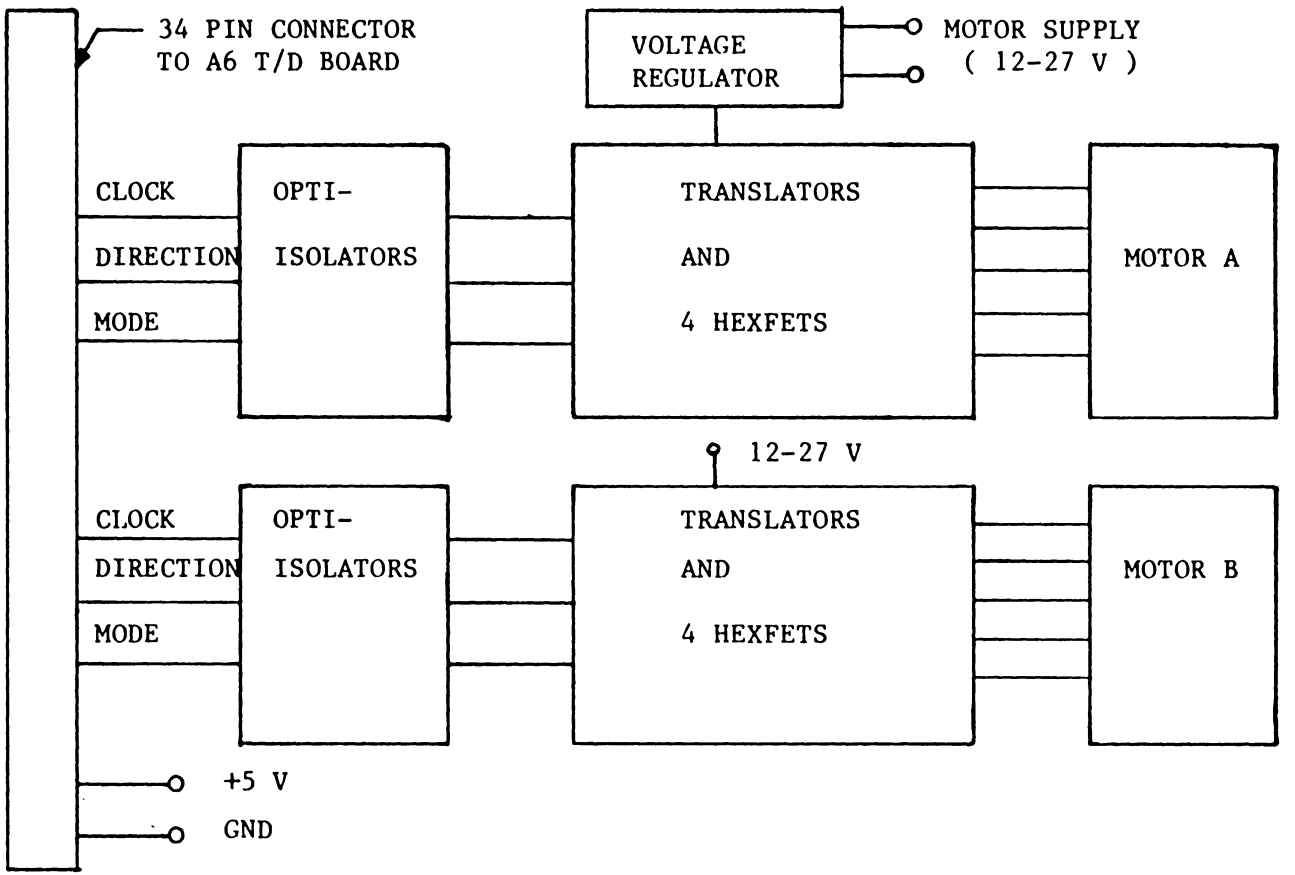

Figure 8. Block Diagram of the R2D23 Board

sisted of timing, refreshing, and interrupt, command-receiver, address registers, address descramble and array soak, transmitter interrupt generator, and adder and end-of-frame circuits. The other section contained an asynchronous communication interface adapter (ACIA) which manipulated and transferred the picture data to the microcomputer.

The ACIA was comprised of a data register and a status register. Information such as start and stop bits of a byte (a computer word consisting of 8 bits), clocking, and parity could be changed by writing to the status register. The status register was used to reset the ACIA by writing a Ø3 Hex to it and to specify the "transmit protocol" which included 1 start bit, 1 stop bit, 8 data bits and the external clock by writing a 14 Hex to it. When bit Ø of the status register was set to 1 it indicated that the data has been received from the camera and could be accessed by reading the data register. When bit 1 of status register was set to 1 a command could be sent to the camera by writing to the data register. The status and the data registers could be accessed by the microcomputer through addresses CØnE and CØnF Hex, where n was the Apple II slot number for the control board plus 8.

In order to protect the microcomputer from moisture and rain and retain a reliable communicaton link with the camera, the control board was divided into two parts and reconnected by five extension wires. The part controlling the camera (Section 1) was mounted on the back of the CLP and the other part (Section 2) was left in the microcomputer. An alternative solution, besides the above solution to the rain problem, was to leave the control board in the microcomputer and increase the length of parallel bus conductors between it and the camera. The idea

was not used since the chances for losing data over a long bus were much more than losing serial data over a long wire.

4.1.2.2 Motor Control Circuitry

The A6 Timer/Driver (A6 T/D) board was a pulse generator which could interface the stepper motor with an Apple II microcomputer. The A6 T/D used two 6840 programmable timer modules (PTMs) to perform the counting, timing, and pulse generation. The counters responded to both internal and external clock signals and could generate an output waveform, a computer interrrupt request signal, or both. Each PTM consisted of 3 binary counters, 3 control registers and one status register. Half of the 16 addresses in the board slot were used by each timer chip. Six of the eight addresses were used for loading the data into the data latches of the timers and the other two were shared by the 3 control registers. Table 5 (Rogers Labs, Inc., Table 5-3) illustrates the relative addresses for 2 PTMs where X (the base counter address) was shown in Table 6 (Rogers Labs, Inc., Table 5-2). A and B used in Table 5, were the two "sides" provided by A6 T/D board for connection to 2 stepper motors.

TABLE 5

A6 T/D PTM Relative Addresses

RELATIVE ADDRESS	FUNCTION	
	READ	WRITE
x + 0/8	Not Used	A/B Control Register 1 or 3
x + 1/9	A/B Status Register	A/B Control Register 2
x + 2/10	A/B MSB Timer 1	A/B MSB Buffer 1
x + 3/11	A/B LSB Buffer 1	A/B LSB Timer 1
x + 4/12	A/B MSB Timer 2	A/B MSB Buffer 2
x + 5/13	A/B LSB Buffer 2	A/B LSB Timer 2
x + 6/14	A/B MSB Timer 3	A/B MSB Buffer 3
x + 7/15	A/B LSB Buffer 3	A/B LSB Timer 3

TABLE 6

A6 T/D Base Counter Addresses

SLOT NUMBER	BASE COUNTER ADDRESS (X)	LATCH ADDRESS
1	49296	49408 - 49643
2	49312	49644 - 49919
3	49328	49920 - 50275
4	49344	50176 - 50431
5	49360	50432 - 50687
6	49376	50688 - 56943
7	49392	50944 - 52299

The control registers set the timers to operate continuously, enabled or disabled their outputs and the interrupt request, and initialized the latch and the counters. Initializing a counter transferred the data from the latches into the control registers and started decrementing as it sensed a clock edge. In continuous operation mode, the counter loaded the data in its latches and started counting down. When it reached zero, it was reinitialized and started decrementing again. This process was repeated and thus produced a continuous square wave.

A quad latch (74LS174) provided four programmable outputs which were either "TRUE" or "FALSE" and were used for stepper motor control. If the A6 T/D board had to drive 4 motors, all the latch outputs would be used for direction control of the motor. If only 2 motors were driven by the board, 2 latch outputs were used for direction control and the other 2 for full- or half-step mode control.

Four DIP switches were used in the A6 T/D board to offer a variety of applicatons. Switches 1 and 2 (SW1 and SW2) were used with the A side and SW3 and SW4 with the B side. When SW1/SW3 was closed (SW2/SW4 open) all three timer outputs were available independently. When SW1/SW3 and SW2/SW4 were closed each side of the board could drive 2 stepper motors in the non-ramp mode. For this application, counters 1 and 2 of each timer (side A and B) "gated" the pulses generated by counter 3 for each of the motors. With SW1/SW3 open and SW2/SW4 closed, side A or B could drive one motor in the ramp mode. Counter 3 supplied the pulses and counter 2 generated end-of-step interrupts. Counter 1 could be used to monitor separate pulses (e.g., pulses generated by

shaft encoderes, etc.). SW1 was opened and SW2 was closed to use side A single motor with ramping capability.

Eight LEDs were utilized for troubleshooting and program development. LEDs 5/1 and 6/2 monitored the output signals of the clocks 2/4 and 1/3. LEDs 7/3 and 8/4 indicated the presence of an input signal on encoder 2/3 and 1/4 on the A/B side.

Applications of the eight jumpers on the board are described below:

H1 - H2	Used when APPLE power supply was used
H3 - H4	Interrupt request line
H5 - H6	Used when R2D23 board was used (optoisolators power supply)
H7 - H8	Auxiliary ground
H9 - H10	Inverted output polarity of Clock 4
H11 - H12	Inverted output polarity of Clock 3
H13 - H14	Inverted output polarity of Clock 2
H15 - H16	Inverted output polarity of Clock 1.

The H5-H6 jumper was used since the R2D23 board was utilized.

A 34 conductor ribbon cable transmitted the signals generated by the A6 T/D board to the motor. The A6 T/D board could drive two stepper motors through the R2D23 board. The R2D23 board consisted of the decoding circuitry and power drivers, the power supply for the A6 T/D logic board, and terminal strips for connection to the motors. The board isolated the A6 T/D board and the microcomputer from motor noise by optical isolators. It also provided input connections for two shaft encoders. A voltage supply of 12 up to 27 VDC with a current output of 2 amps was required to power the board.

4.2 PRINCIPLE OF OPERATION

The profiler which was developed used similar triangles principle for soil surface height measurements as illustrated in Figure 9. The laser beam was reflected from the soil surface, focused by the lens, struck the Optic RAM surface and discharged a number of capacitors towards zero volts. The number of capacitors discharged depended on the size of the lens opening and size and intensity of laser beam. The distance between capacitors discharged and the center of the RAM (NP) changed in an inverse fashion with the change in the distance between the soil surface and the lens plane (H). Height H was calculated at different points over the soil surface from the relation:

$$H = FL/NP \tag{2}$$

where:

F - distance between lens and optic RAM planes

L - distance between laser beam and lens axis

P - distance between alternate pixels in a row

N - number of pixels (capacitors) between centers of optic RAM and discharged capacitor.

Distances F and L were kept fixed after being determined by error analysis and could be measured by a caliper or ruler. P was given (Table 1) to be equal to 0.0215 mm for the distance between two capacitors in a row) or 0.043 mm (for the distance between alternate capacitors in a row). Distance NP was found from the software. The

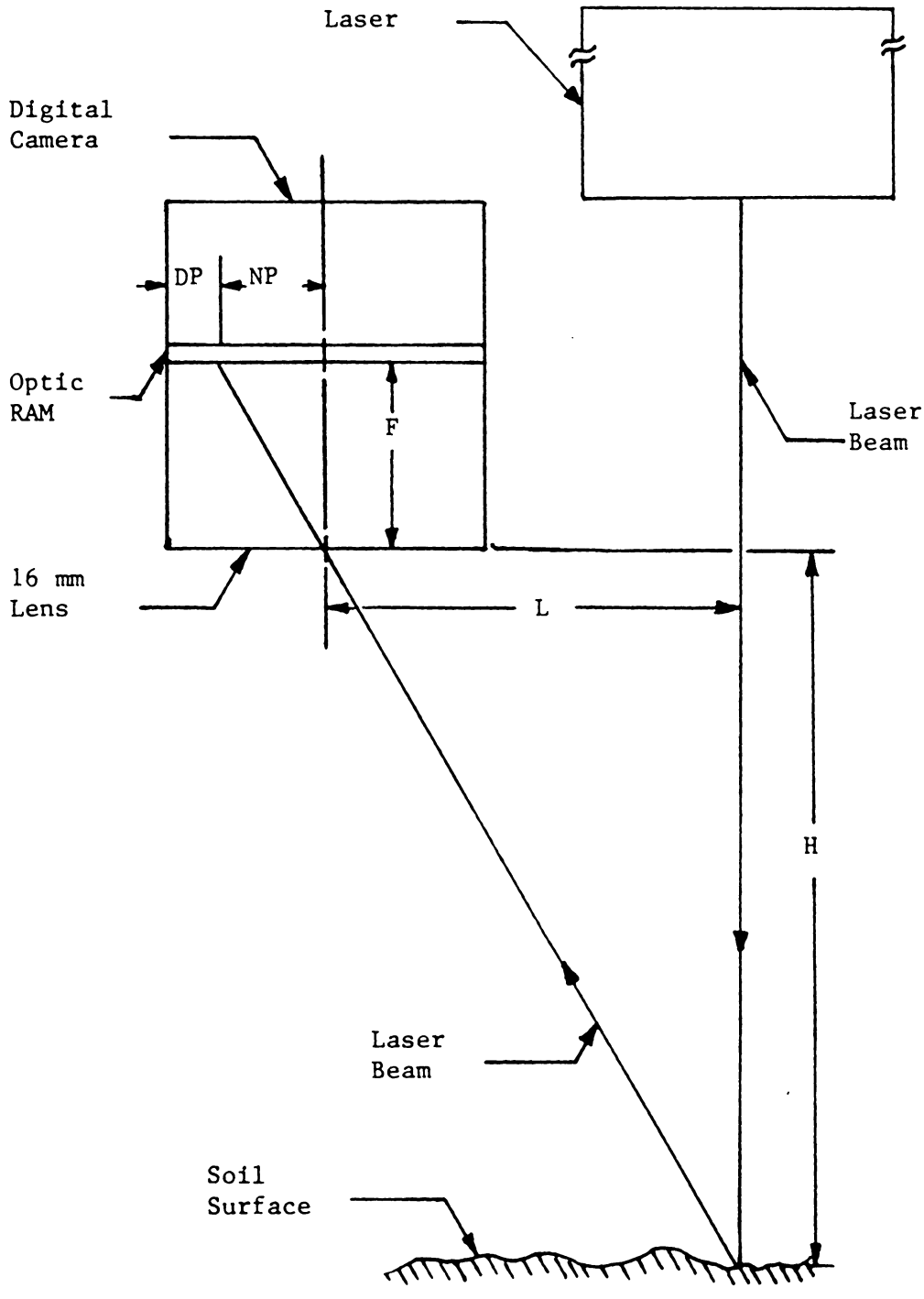

Figure 9. Principle of Height Measurement

procedure was to first find the number of capacitors between the center of the discharged capacitors (pixels) and the left edge of the RAM (D). Then subtract D from half the number of alternating capacitors in a row (depending on picture size) to find N. And finally multiply N by P to come up with NP.

4.3 CONTROL SOFTWARE

The software developed to control the camera and motor operations and to calculate the soil surface heights was written in FORTH. The FORTH language was preferred over other commercially available languages (e.g., BASIC, FORTRAN, etc.) because of its speed (somewhat slower than assembly, but much faster than BASIC or others), compactness, versatility (user's definition provisions), and ease of use. The programs were written based on an understanding of the camera and motor hardware and operation and mathematics of height measurements.

4.3.1 Camera Control Software

The digital camera could operate in several modes as specified by the command byte written into the status register of the ACIA. A command byte has the following organization:

Bit 0	0, SEND mode
	1, NO SEND mode
Bit 1	0, REFRESH mode
	1, SOAK mode
Bit 2	0, 1ARRAY mode
	1, 2ARRAY mode
Bit 3	0, 7BIT mode

	1, 8BIT mode
Bit 4	0, wide pixel mode (WIDEPIX)
	1, no-wide pixel mode (NOWIDPIX)
Bit 5	0, Alternating bit mode (ALTBIT)
	1, No alternating bit mode (NOALTBIT)
Bit 6	Always 1
Bit 7	Always 1

In ALTBIT mode camera transmited only from even rows and alternate columns of pixels while in NOALTBIT mode all the data were transmitted to the microcomputer.

WIDEPIX mode maintained the proper ratio between height and width of the picture by double transmitting the pixels.

7BIT mode was only used for Apple graphics. This mode made the camera transmit a byte with 7 data bits and a color bit. The 8BIT mode was the alternate option which was used in other microcomputers' graphics and non-graphics modes. It could also be used in Apple's non-graphic mode.

1ARRAY mode used only one of the two 128 x 256 pixel arrays.

In the REFRESH mode capacitors were charged up to 5 volts while the camera was transmiting an image. When capacitors were not refreshing, they were said to be in the SOAK mode. The SOAK mode allowed the capacitor charges to leak away at a rate proportional to the intensity of the light focused on them. The SOAK mode was invoked automatically when the camera ended the transmission of an image and was retained until another command was received.

TABLE 7

Command Required for Different Picture Sizes

MODE SELECTION	ROWS	BYTES PER ROW	PIXELS PER ROW	COMMAND (HEX)	(DEC)
ALTBIT WIDPIX	64	37	256	CO	192
ALTBIT NOWIDPIX	64	19	128	DO	208
NOALTBIT WIDPIX	128	73	512	EO	224
NOALTBIT NOWIDPIX	128	37	256	FO	240

The SEND mode was invoked by setting bit 0 of command byte equal to 0 which initiated the transmission of an image. If bit 0 of the command byte was set to 1, the camera did not transmit any image and refreshed or soaked depending on the status of the second bit (bit 1) of the command byte. When SEND bit was set to 1, bit 4 also needed to be set to 1 in order to prevent a 1-bit-offset of the next picture image.

Table 7 shows the commands needed to obtain different pictures in 1ARRAY and 7BIT modes. Camera control software is shown in Appendix A.

4.3.2 Motor Control Software

The motor control software was also written in FORTH and is listed in Appendix B. The software communicated with the A6 T/D board by utilizing the 16 addresses provided by the Apple II slot for the board (Tables 5 and 6). Eight of the addresses were used by the PTM chip of the A side and the remaining eight by the PTM chip of the B side. Different functions were performed by the A6 T/D board by accessing the related timer and its control registers. The 3 control registers controlled the operation of the timers by writing a command byte into them. The command byte configuration is shown below.

Bit 0 (Register 1)

0, all timers can operate

1, all timers in preset state

(Register 2)

0, counter 3 can be written into

1, counter 1 can be written into

(Register 3)

0, clock not prescaled

1, clock presealed by 8

Bit 1 0, timer 1, 2 or 3 using external clock

1, timer 1, 2 or 3 using enable clock

Bit 2 0, timer 1, 2 or 3 16-bit mode

1, timer 1, 2 or 3 8-bit mode

Bit 3 Interrupt control and timer 1, 2 or 3 counter mode

Bit 4 Interrupt control and timer 1, 2 or 3 counter mode

Bit 5 Interrupt control and timer 1, 2 or 3 counter mode

Bit 6 0, interrupt flag masked on $\overline{IRQ}$.

1, interrupt flat enabled on $\overline{IRQ}$.

Bit 7 0, timer output masked on output (1, 2, or 3)

1, timer output enabled on output (1, 2, or 3)

4.3.3 Height Calculation Software

Height calculation software was written in FORTH based on Equation (2). Distances F and L were measured by a caliper and were equal to 16 and 21 mm, and distance p was equal to 0.043 mm as given in Table 1. For each height calculation, a picture of the laser beam reflected from the soil surface was taken. The picture was then simultaneously stored in the first graphics page of Apple II memory and was displayed. The number of pixels between the center of the Optic RAM and the center of

the light pixels, N, was found from the stored data. The height H was then calculated by having all the parameters in Equation (2).

Only half of the 256 pixels for each row of the RAM could be used for height calculations. Pixels in the right half of the RAM could not be accessed due to the geometry of the camera as seen in Figure 9. The total number of usable pixels in the left half was reduced to 64 when operating the camera in the ALTBIT mode. Figure 10 illustrates a 128 bits per row x 64 rows (19 bytes per row x 64 rows) picture of the laser beam as stored in the first graphics page of Apple II memory and displayed on the screen.

Since more than one pixel was discharged by the laser beam light, N had to be calculated by finding the average of N's for the rows containing the light pixels. Calculation of N for each row could be carried out by scanning the picture (Figure 10) from either right to left or left to right. Since it was easier to write the software for a left-to-right scanning procedure, that algorithm was used. In the left-to-right scanning procedure, N could be found from:

$$N_i = 64 - D_i \tag{3}$$

where:

N_i - number of pixels between center of the picture and the center of the light pixels in row i

D_i - number of pixels between left edge of the picture and the center of the light pixels in row i

64 - number of pixels per row in the left half of the array.

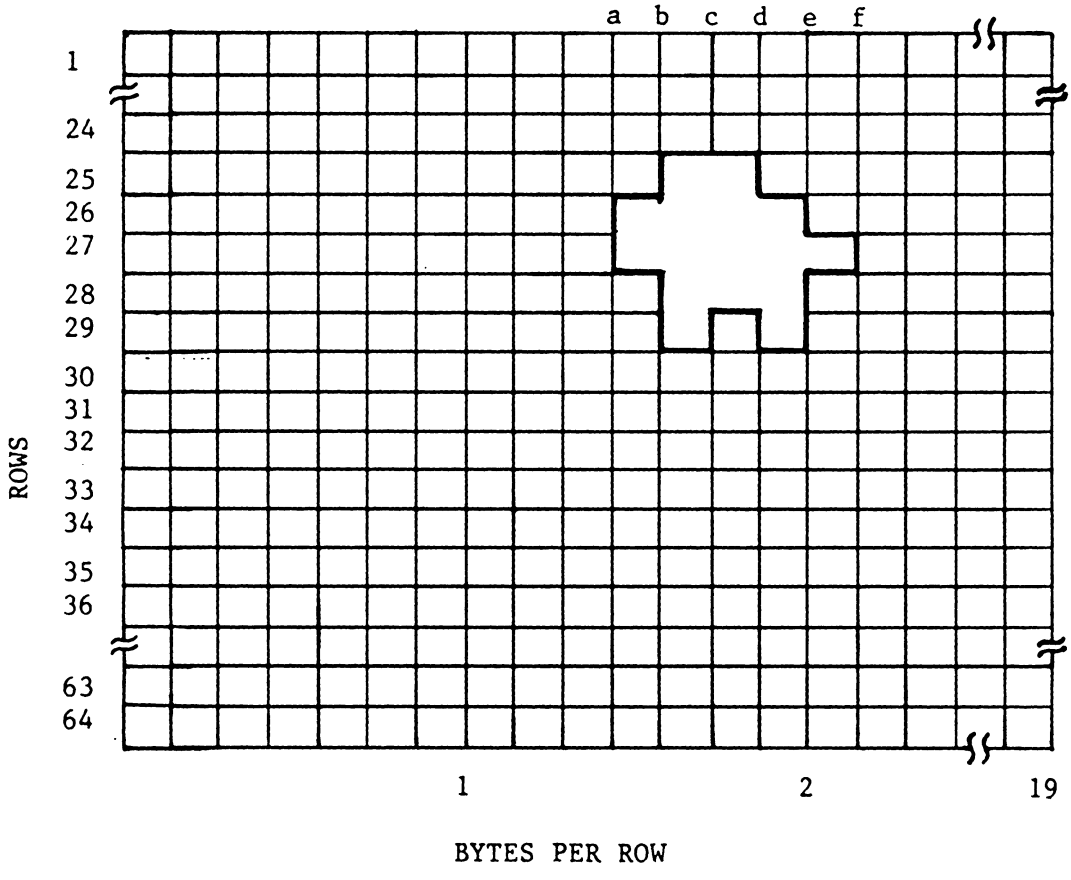

Figure 10. A 128 x 64 Picture of the Laser Beam as Displayed on the Screen of Apple II

In scanning the picture, each row of pixels could be accessed by individual bytes (7 bits) and each byte by single bits. In order to facilitate calculation of N_i, an attempt was made to modify equation (3) to include the number of light pixels in a row ($BITCNT_i$), sum of position of the light pixels in the byte(s) containing them (SUM_i), and the number of remaining bytes between the byte(s) containing the light pixels and the left edge of the picture ($NOBYTE_i$). The modified equation was:

$$N_i = 64 - [7(NOBYTE_i) + (SUM_i)/(BITCNT_i) - 1/2] \qquad (4)$$

where:

64 - number of usable pixels in each row in the left half of RAM (ALTBIT mode)

$7(NOBYTE_i)$ - number of dark pixels between the left edge of RAM and the byte(s) containing the light pixels

$(SUM_i)/(BITCNT_i) - 1/2$ - number of pixels (light and/or dark) between the byte(s) not containing any light pixels and the center of the light pixels.

Since pixel number (or position of a pixel in a byte) was $1/2$ a unit bigger than the number of pixels and $(SUM_i)/(BITCNT_i)$ pointed to the position of the center line of light pixels, a $1/2$ had to be subtracted from it to convert the position to number of pixels.

The values of N_i for rows 25, 26, 27, 28, and 29 of Figure 10 are listed below using distances a,b,...,f.

$$N_{25} = 64 - [b + (d - b)/2] \tag{5}$$

$$N_{26} = 64 - [a + (e - a)/2] \tag{6}$$

$$N_{27} = 64 - [a + (f - a)/2] \tag{7}$$

$$N_{28} = 64 - [b + (e - b)/2] \tag{8}$$

$$N_{29} = 64 - \{[b+(c-b)/2](c-b)+[d+(e-d)/2](e-d)]\}/[(c-d)+(e-d)] \tag{9}$$

Validity of Equation (4) could be checked by substituting the numerical values of a through f into Equations (5) through (9) and comparing the results with the N_i's obtained from Equation (4). For row 25 in Figure 10 values of $NOBYTE_{25}$, $BITCNT_{25}$ and SUM_{25} were equal to 1, 2 and 11 (5 + 6). Substituting into Equation (4) resulted in:

$$N_{25} = 64 - [(1)(7) + (5 + 6)/2 - \tfrac{1}{2}] = 52$$

where using Equation (5) resulted in:

$$N_{25} = 64 - [11 + (13 - 11)/2] = 52$$

which checked with N_{25} obtained by Equation (4). By a similar procedure, N_{26} was found from Equation (4) to be equal to:

$$N_{26} = 64 - [(1)(7) + (4 + 5 + 6 + 7)/4 - \tfrac{1}{2}] = 52$$

which agreed with:

$$N_{26} = 64 - [10 + (14 - 10)/2] = 52$$

obtained from Equation 6). The difference between row 27 and rows 25 and 26 was that the light pixels in row 27 belonged to more than one byte (bytes 2 and 3). Values of $NOBYTE_{27}$, $BITCNT_{27}$ and SUM_{27} were found from Figure 10 to be equal to 1, 5 and 30(4 + 5 + 6 + 7 + 8). The value of N_{27} obtained from Equation (4) was:

$$N_{27} = 64 - [(1)(7) + (30)/5 - \tfrac{1}{2}] = 51.5$$

and the value of N_{27} from Equation (7) was:

$$N_{27} = 64 - [10 + (15 - 10)/2] = 51.5$$

which were the same.

Calculation of N_{28} was similar to that of N_{25} and N_{26} since the light pixels belonged to only one byte (byte 2). The arrangement of light pixels in row 29 was different than rest of the rows. The difference in row 29 was accounted for in Equation (10). Using Equation (10), N_{29} was found to be:

$$N_{29} = 64 - \{[11 + (12-11)/2]\,(12-11) + [13 + (14-13)/2](14-13)\}/[(12-11) + (14-13)] = 51.5$$

which matched with N_{29} obtained from Equation (4).

$$N_{29} = 64 - [(1)(7) + (5 + 7)/2 - 1/2] = 51.5$$

The overall N could be calculated from:

$$N = \sum_{i=1}^{64} [(N_i)(BITCNT_i)] \; / \; \sum_{i=1}^{64} (BITCNT_i) \qquad (10)$$

where:

N_i - N calculated for each row containing the light pixels

$(BITCNT_i)$ - number of light pixels per row

$\sum_{i=1}^{64} (BITCNT_i)$ - total no. of light pixels in a picture (TOTBIT).

Substitution of Equation (4) into Equation (10) yielded:

$$N = \Big[\sum_{i=1}^{64} [64 - [7(NOBYTE_i) + (SUM_i)/(BITCNT_i) - 1/2]] \, (BITCNT_i) \Big] \; / \; \sum_{i=1}^{64} (BITCNT_i) \qquad (11)$$

which when expanded and rearranged resulted in:

$$N = \sum_{i=1}^{64} [(64 + 1/2)\ (BITCNT_i)\ ] \ /\ \sum_{i=1}^{64} (BITCNT_i)$$

$$- \sum_{i=1}^{64} [7(NOBYTE_i)\ (BITCNT_i)\ ] \ /\ \sum_{i=1}^{64} (BITCNT_i) - [\sum_{i=1}^{64} [(SUM_i)$$

$$/(BITCNT_i)\ ]\ (BITCNT_i)\ ]\ /\ \sum_{i=1}^{64} (BITCNT_i) \qquad (12)$$

and when simplified yielded:

$$N = 64.5 - 7 \sum_{i=1}^{64} [(NOBYTE_i)\ (BITCNT_i)]/(TOTBIT)$$
$$- [\sum_{i=1}^{64} (SUM_i)]/(TOTBIT) \qquad (13)$$

which could be further reduced to :

$$N = 64.5 - [\sum_{i=1}^{64} [7\ (NOBYTE_i)\ (BITCNT_i) + (SUM_i)]]/(TOTBIT) \qquad (14)$$

or:

$$N = 64.5 - TERM/TOTBIT \qquad (15)$$

where:

$$TERM - \sum_{i=1}^{64} [7\ (NOBYTE_i)\ (BITCNT_i) + (SUM_i)]$$

and:

$$TOTBIT - \sum_{i=1}^{64} (BITCNT_i)\ .$$

The software written for height calculations using Equations (2) and (14) is shown in Appendix C. Figure 11 shows the flow diagram of the software.

4.4 ERROR ANALYSIS AND CALIBRATION

The sources of error in the of height measurement were rod deflection, light reflectivity of the soil surface, vertical distance between the profiler and the soil surface, and errors in estimating parameters N, p, L, and F of Equation (2). The sources of error affecting the horizontal movement were motor shaft slippage, gear slippage, chain vibration, rod deflection, and ball bearing misalignment. An error analysis was required to determine the amount of error contributed by the parameters in Equation (2) to the height measurement error and a calibration was necessary to minimize the overall system error. Since there was not adequate information available for the sources of error affecting the horizontal movement, no error analysis was performed. The device was calibrated to test its displacement repeatability.

4.4.1 Error Analysis

An error analysis was performed to estimate the theoretical values of error resulting from parameters in Equation (2), to determine the overall height measurement error, and to improve the accuracy by choosing the proper values for F, L, P and N (Doebelin, 1983). The

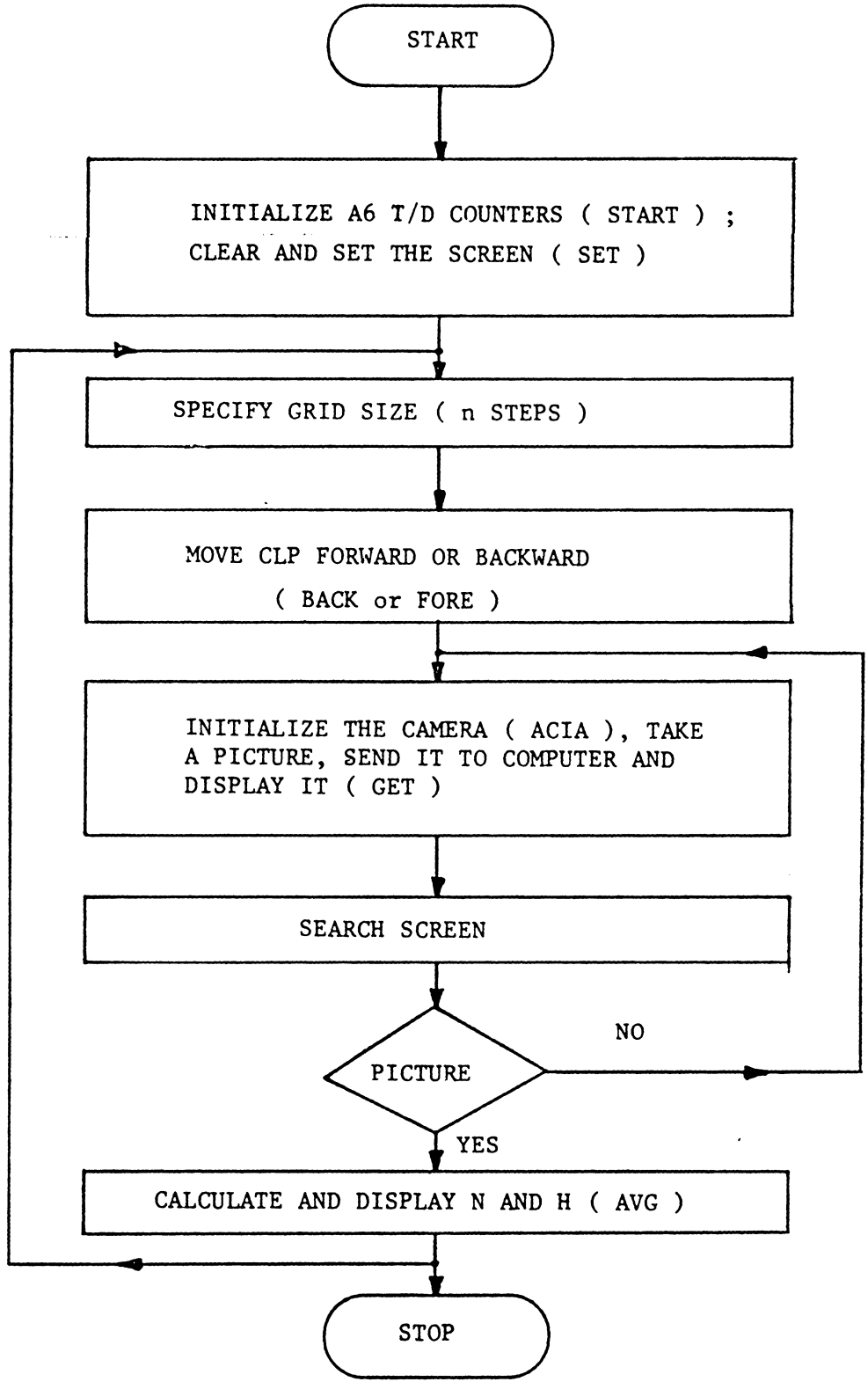

Figure 11. Flow Diagram of the Control Software

error terms pertaining to F, L, N and P were obtained by taking the partial derivative of H with respect to each parameter and multiplying it with the expected measurement error of that parameter (Δ). The error terms are listed as follows:

$$E_F = \left|\frac{\partial H}{\partial F}\right| \ |\Delta F| = \left|\frac{L}{Np}\right| \ |\Delta F| \tag{16}$$

$$E_L = \left|\frac{\partial H}{\partial L}\right| \ |\Delta L| = \left|\frac{F}{Np}\right| \ |\Delta L| \tag{17}$$

$$E_N = \left|\frac{\partial H}{\partial N}\right| \ |\Delta N| = \left|\frac{-LFP}{(Np)^2}\right| \ |\Delta N| \tag{18}$$

$$E_p = \left|\frac{\partial H}{\partial p}\right| \ |\Delta p| = \left|\frac{-LFN}{(Np)^2}\right| \ |\Delta p| \tag{19}$$

where E_F, E_L, E_N and E_P are errors due to F, L, N, and P.

The distances F and L could be measured with an accuracy of ±0.5 mm, therefore ΔF and ΔL were set to be equal to ±0.5 mm. Since there was no information given by the RAM manufacturer for the measurement error of p the value of Δp was assumed to be equal to 1 percent of p (±0.0004 mm for ALTBIT mode and ±0.0002 mm for NOALTBIT mode). The value of ΔN was equal to one-half of a digit or ±0.5.

In order to minimize the magnitude of errors (E_F, E_L, E_N, and E_p), F and L had to be chosen as small as feasable and N and p as large as possible. The focal length of the lens (F), and the distance between pixels (p) for ALTBIT and NOALTBIT modes had fixed values of 16, 0.043 and 0.0215 mm, respectively. The smallest value for L (21 mm) was obtained by installing the laser and the camera as close together as

physically possible. Since F, L, and p were constant, the only parameter influencing the magnitudes of error was the variable N and the error decreased as the value of N increased.

The numerical values of the error terms were calculated for 4 different heights (150, 200, 250, and 300 mm) for both ALTBIT and NOALTBIT modes of the camera. N was computed for different height using Equation (2) by assigning values for F, L, and p equal to 16, 21, and 0.043 or 0.0215 mm depending on the mode. The values of N, p, F, L, ΔN, Δp, ΔF, and ΔL were then substituted into Equations (16) through (19) which yielded the values of E_L, E_F, E_p, and E_N as shown in Tables 8 and 9.

The overall error, E_{rss}, was calculated utilizing the root sum square (rss) formula:

$$E_{rss} = \left[\left(\frac{\partial H}{\partial F}\Delta F\right)^2 + \left(\frac{\partial H}{\partial L}\Delta L\right)^2 + \left(\frac{\partial H}{\partial N}\Delta N\right)^2 + \left(\frac{\partial H}{\partial p}\Delta p\right)^2\right]^{1/2} \qquad (20)$$

and the percentage of overall error, % E_{rss}, was calculated relative to H. The values of E_{rss} and % E_{rss} for both operation modes of the camera are listed in Table 10.

4.4.2 Calibration

Calibration of the profiler was required to minimize the overall height measurement error and to develop a model including the error term based on Equation (2). Calibration was also necessary to determine the effect of light reflectivity of soil, vertical distance between the soil surface and the profiler, and rod deflection on the accuracy of height

TABLE 8

Error Terms at Different Heights for the 16 mm Camera in ALTBIT Mode

H (mm)	N	E_F (mm)	E_L (mm)	E_N (mm)	E_P (mm)
150.3	52	4.7	3.6	1.4	1.4
200.4	39	6.3	4.8	2.6	1.9
252.1	31	7.9	6.0	4.1	2.3
300.5	26	9.4	7.2	5.8	2.8

TABLE 9

Error Terms at Different Heights for the 16 mm Camera in NOALTBIT Mode

H (mm)	N	E_F (mm)	E_L (mm)	E_N (mm)	E_p (mm)
150.3	104	4.7	3.6	.72	1.4
200.4	78	6.3	4.8	1.3	1.9
252.1	62	7.9	6.0	2.0	2.3
300.5	52	9.4	7.2	2.9	2.8

TABLE 10

E_{rss} and % E_{rss} for the Camera With the 16 mm Lens in ALTBIT and NOALTBIT Modes

H (mm)	E_{rss} (mm) ALTBIT	E_{rss} (mm) NOALTBIT	% E_{rss} ALTBIT	% E_{rss} NOALTBIT
150.3	6.2	6.1	4.1	4.1
200.4	8.5	8.2	4.2	4.1
252.1	10.9	10.4	4.4	4.1
300.5	13.4	12.5	4.5	4.2

measurements. A second calibration was necessary to examine the horizontal movement repeatability of the profiler and to find the relationship between the displacement and the number of motor steps.

4.4.2.1 Height Measurement Calibration

Height measurement calibration was performed by utilizing an artificially colored and shaped surface. An aluminum block with seven 1.5 cm steps was constructed to represent the different soil surface heights. The surface of steps was covered with a black and a white tape to simulate the maximum and the minimum degrees of light reflectivity. An adjustable metal stand, ranging in height from 35 to 55 cm in 5 cm increments, was built to offer more flexibility in surface heights.

The profiler was placed on the metal stand on a flat table in a laboratory. The distance between the camera lens and the table surface was measured by a steel tape at three locations along the profiler. The distances were 27.43, 27.31, and 27.43 cm at the motor end, the center, and the gear end of the profiler, respectively. The distance between each step and the camera lens (MH) was calculated by measuring the step size by a caliper and subtracting it from the original height at each location. The distances for each step at each location were calculated once, assuming that the rod deflection was repeatable in all trials.

The height measurement for calibration was accomplished by writing a short FORTH program which utilized the 3 previously developed programs. The height measurement software used Equation (2) with F, L and p equal to 16, 21 and .043 mm (ALTBIT mode). Figure 11 represents the flow diagram of the program. The data collection proceeded as

follows. The aluminum block was placed on the table under the CLP at the motor end of the profiler. A picture of the laser beam, relfected from the surface of a step, was taken and displayed on the screen. The number of pixels, N, and the theoretical distance between the step and the lens, TH, were calculated, displayed, and hand-recorded. Then, the motor advanced the CLP to the next block step and stopped for data collection. The process was repeated for all seven steps. The data collection was carried out five times for each color, step, and location. The rate of data collection was 32 points per minute. The data are listed in Appendix D.

4.4.2.2 Horizontal Movement Calibration

Two experimental methods were employed to calibrate the horizontal movement. The first method evaluated the error associated with small number of motor steps and determined the relationship between motor steps and horizontal travel. The second method determined the overall error in horizontal displacement.

In the first experiment a dial indicator (Starrett Universal Dial Test Indicator No. 196) was used to measure the distance moved by CLP due to a small number of motor steps. The dial indicator was attached to the base of the metal stand at the motor end and the edge of CLP was put in contact with the spring-loaded needle of the dial. The CLP was displaced horizontally equivalent to one motor step and the dial reading was taken. The data were collected for seven such displacement steps. This measurement procedure was repeated 4 times at each of the 3 locations along the profiler.

In the second experimental method the dial indicator was mounted on the metal stand base at the motor end of the profiler. The dial needle was then pressed in by the CLP and the dial was set to zero. The CLP was moved away and back in contact with the needle with the same number of motor steps. The deviation of the dial from zero was recorded for 50 steps (approximately 1 cm) up to 4000 steps (about 70 cm). The measurements were repeated twice at both the motor and the gear ends of the profiler. The data are shown in Appendix E.

4.5 DATA ANALYSIS AND DISCUSSION

4.5.1 Data Analysis

Three non-linear models similar to that of Equation (2) were fit to the data collected for height calibration. The models were:

$$MH = \frac{k_1}{k_2 - D} + k_3 + e \tag{21}$$

$$MH = \frac{k_1}{k_2 - D} + e \tag{22}$$

$$MH = \frac{k_1}{64 - D} + k_2 + e \tag{23}$$

where:

MH - measured height of each step (measured manually)

D - number of pixels between the left edge of the RAM and the center of the light pixels

k_1, k_2, k_3 - constants representing F, L, and p

e - random error.

Table 11 lists the residual mean square (RMS) for each model using the data in different combinations of colors and locations.

The 4 sets of calibration data for horizontal displacement utilizing the first experimental method, were first averaged and converted to mm. Then a linear regression model was fit to the data. The model was:

$$x = n\ s + e \tag{24}$$

where:

- x - horizontal distance traveled by the CLP (theoretical)
- s - horizontal distance (equal to one motor step) traveled by CLP (measured)
- n - number of motor steps
- e - random error.

The model did not have an intercept since for zero motor steps there was no CLP movement. Table 12 lists the estimated values of S and its standard error obtained from the statistical analysis of the data at the motor end, the center, and the gear end of the profiler.

Similar displacemnt data collected using the second experimental method were expressed in mm and the mean and the standard deviations were calcualted for each set of data. Table 13 lists the results.

Figures 12 and 13 illustrate the error vs. number of steps for the motor end and the gear end of the profiler, respectively.

TABLE 11

A Comparison Between Residual Mean Squares(RMS) of Model 1 (Equation (21)), Model 2 (Equation (22)), and Model 3 (Equation (23)) Using the Camera with the 16 mm Lens

COLOR	POSITION							MODEL
	1	2	3	1&2	1&3	2&3	1&2&3	
BLACK	.0067	.0078	.0070	.0075	.0066	.0081	.0075	1
WHITE	.0087	.0031	.0062	.0085	.0120	.0049	.0095	1
B&W	.0089	.0077	.0085	.0086	.0101	.0085	.0043	1
BLACK	.0066	.0077	.0071	.0075	.0067	.0082	.0076	2
WHITE	.0097	.0036	.0082	.0095	.0140	.0061	.0110	2
B&W	.0090	.0076	.0086	.0086	.0103	.0086	.0095	2
BLACK	.0067	.0077	.0069	.0076	.0067	.0081	.0076	3
WHITE	.0130	.0054	.0108	.0120	.0172	.0082	.0130	3
B&W	.0105	.0085	.0098	.0099	.0118	.0096	.0107	3

TABLE 12

Statistical Results for Horizontal Movement
Calibration Obtained from the Data for the First Method

LOCATION	ESTIMATE OF S (mm)	STANDARD ERROR (mm)
MOTOR END	0.175	0.00155
CENTER	0.175	0.00170
GEAR END	0.175	0.00221

TABLE 13

Mean and Standard Deviation of the Data
Collected by the Second Method for Horizontal Calibration

LOCATION	TRAIL	MEAN (mm)	STANDARD DEVIATION (mm)
MOTOR END	1	-0.0051	0.040
GEAR END	1	0.0055	0.023
MOTOR END	2	0.00096	0.058
GEAR END	2	0.011	0.024

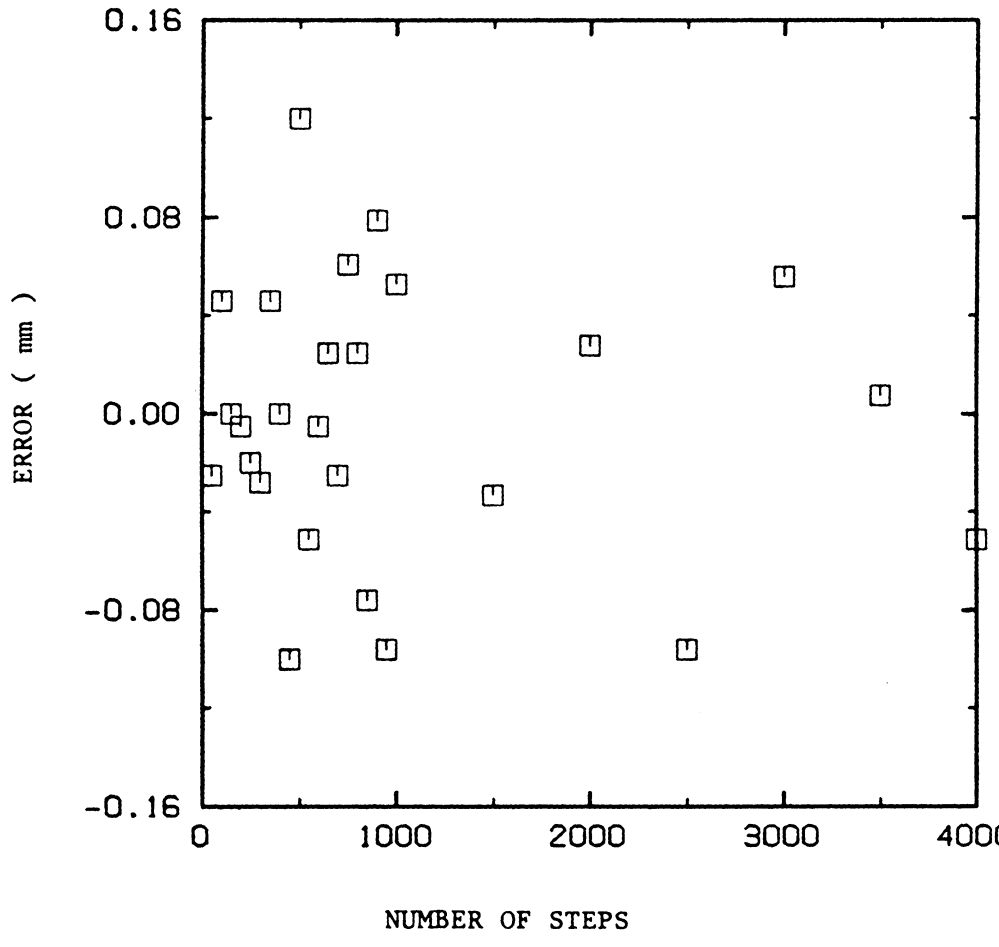

Figure 12. Error vs. Number of Steps at the Motor-end of the Profile Meter

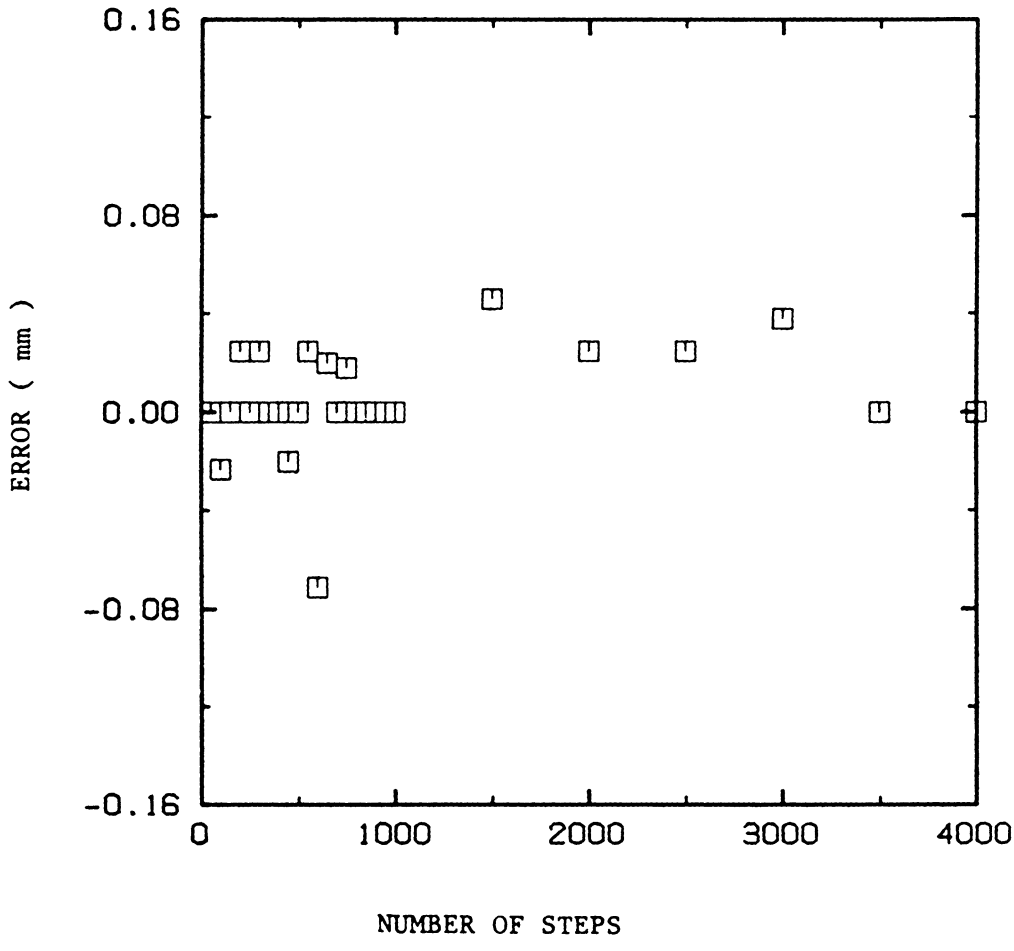

Figure 13. Error vs. Number of Steps at the Gear-end of the Profile Meter

4.5.2 Discussion

The results of error analysis listed in Tables 8 and 9 indicate that as the height H became larger, the distance Np decreased and the overall error and the individual errors increased. The increase in error resulted from the nonlinearity of Equation (2). Tables 8 and 9 also show a decrease in the magnitude of error produced by F, L, N, and p, respectively, as distance decreased. The errors due to the estimation of F, L, and p were minimized by calibration while the error resulting from N was not.

A comparison of the residual mean squares (RMS) for the 3 models listed in Table 11 showed that color and location (rod deflection) had no statistically important effect on height measurements and the 3 models were not significantly different. Therefore the simplist model Equation (22), obtained from all the data with k_1 and k_2 equal to 829.0 and 66.4, was selected for later use. The calibrated error of model (2) was calculated to be equal to ±1.95 mm by taking twice the square root of the RMS value (.0095 cm^2) for the whole data as listed in Table 11. Figure 14 illustrates a plot of residual vs. measured height (MH) for the second model (Equation (22)).

The deflection at the center of the rods (worst case) with 2.27 kg load (half the CLP weight on each rod) was measured by a steel tape to be 1.2 mm. The effect of deflection on difference in height measurements at a point was minimal since it was assumed that the rods deflected the same amount at each point every time.

Analysis of the data collected for horizontal movement calibration, presented in Table 12, indicated that each motor step was equal to 0.175

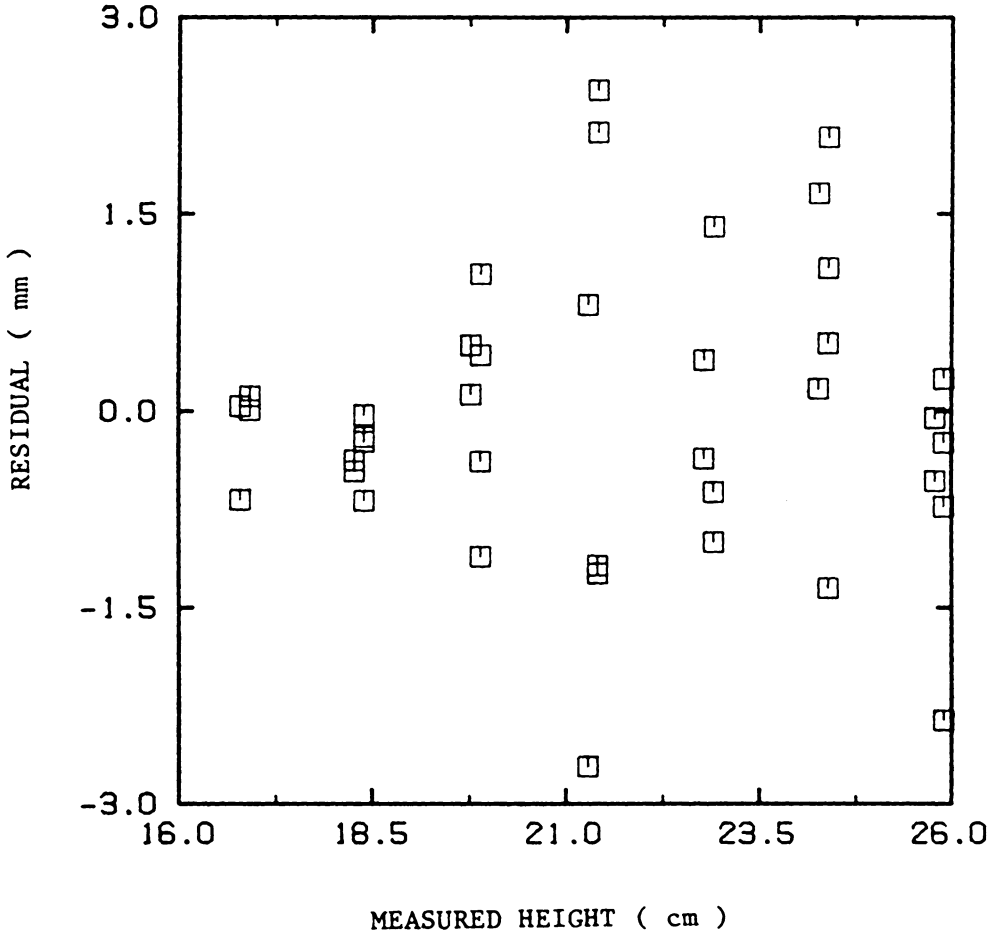

Figure 14. Residual vs. Measured Height
for Equation (22)

mm of CLP travel and the error per step was about 0.0019 at the motor end, the center, and the gear end of the profiler.

The error for the horizontal movement calibration over 70 cm length of the profiler was equal to ±0.12 mm. This error was obtained by multiplying the largest standard deviation in Table 13 (0.058 mm) by 2 for a 95 percent confidence interval. Since the overall error (±0.12 mm) was smaller than the laser beam diameter (0.63 mm), the number of steps multiplied by 0.175 mm could be used to indicate the horizontal position (x coordinate) of the CLP.

The accuracy of the profiler (±1.95 mm), obtained by calibration, did not satisfy the desired accuracy (±1.00 mm). One reason for that was the use of half of the RAM surface. Therefore, redesigning the height measuring unit (basically the camera) was considered as the primary solution to the inaccuracy of the device. A comparison of errors presented in Tables 8 and 9 indicated that E_F, E_L, and E_p were the same for both ALTBIT and NOALTBIT modes while E_N was twice as small for NOALTBIT than ALTBIT mode. Since value of E_N had a decisive effect on the overall error and E_N was smaller for NOALTBIT mode, operating the camera in NOALTBIT mode was considered as another solution to the problem of inaccuracy. Although NOALTBIT was considered as a factor improving the accuracy, it was also considered a factor in reducing the speed of data collection (since the number of pixels per row and number of rows doubled in comparison with ALTBIT).

The speed of data collection (32 points per min) was also less than the speed specified in the design objective (2 points per sec). The factors affecting the speed were the time required to display the data,

the rate of data transfer, the motor speed, and the software efficiency. The speed of operation could be improved by using a faster motor, increasing the baud rate (Table 2) by writing portions of the programs in assembly language, and by receiving only the part of the data which included the laser image information.

Chapter V

DESIGN OF THE NEW CAMERA

5.1 ERROR ANALYSIS

The height measurement error estimate of ±1.95 mm, obtained from analysis of data collected in calibrating the camera with 16 mm lens, was not within the range of the error specified in the design objectives (±1.00 mm), therefore various options were examined to improve the accuracy. Various options were available; usage of the whole surface area of the RAM, installing the RAM in an angle to the lens, substituting a different focal length lens for the 16 mm lens, and operating the camera in the NOALTBIT mode. A comparison of the error inherent in each option was required in order to redesign the camera.

5.1.1 Full vs. Half RAM Surface

In the original camera more than half of the pixels in each row of the RAM could not be utilized which affected the resolution and increased the error. Doubling N could reduce the error since it was in the denominator of the error terms shown in Equations (16) through (19). In the design of the new camera the RAM was shifted a distance d to the left of the axis of the camera allowing the whole surface of the RAM to be used. Figure 15 shows the arrangement of the new camera and the laser.

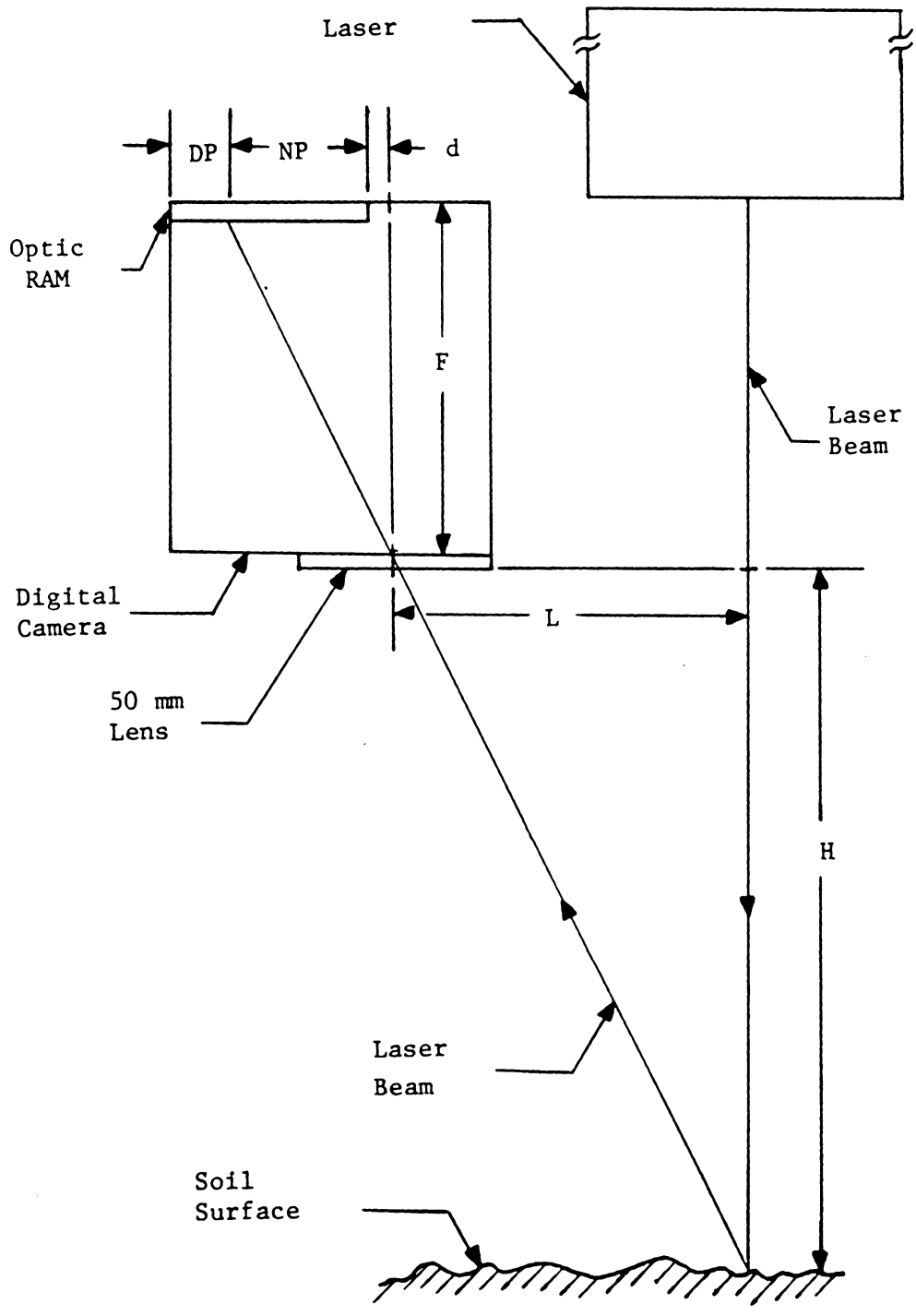

Figure 15. The New Camera and Laser Arrangement

5.1.2 50 mm vs. 16 mm Lens

The error using the 16 mm lens was compared with that using a 50 mm one with the design illustrated in Figure 15. The equation describing the relationship between the height and other parameters shown in Figure 15 was:

$$H = F\ L/(N\ P + d) \tag{25}$$

where:

H, F, L, N, and P - previously defined

d - offset distance between the right edge of the RAM and the camera axis, used as an adjustment variable.

The operating distance between the camera-laser plate and the soil surface (H) was assumed to be 250 mm ±50 mm of soil erosion or deposition. Therefore, Hmin and Hmax had a values of 200 mm and 300 mm, respectively. To proceed with the error analysis, values of L and d had to be calculated from Equation (25) by substituting the values of H, N, P, and F. For the 16 mm lens and the camera at Hmin, Equation (25) resulted in:

$$L = 12.5\ d + 67.19 \tag{26}$$

and substituting values of Hmax, Nmin, P, and F into Equation (25) yielded:

$$L = 18.75\ d + 2.42 \tag{27}$$

Solving Equations (26) and (27) d was computed as 10.36 mm. Substituting for d back into Equation (26) or (27), resulted in an L equal to

196.67 mm. Since more than one pixel formed the width of a laser beam image, 3 and 125 were used in ALTBIT mode (instead of 0 and 128) and 6 and 250 in NOALTBIT mode (instead of 0 and 256) for Hmin and Hmax.

The error associated with parameters in Equation (25) were obtained by taking the derivative of H with respect to each parameter and multiplying it by the Δ (delta) of that parameter. The error terms are listed below.

$$E_F = (L\ \Delta F)/(N\ P + d) \tag{28}$$

$$E_L = (F\ \Delta L)/(N\ P + d) \tag{29}$$

$$E_d = (-F\ L\ \Delta d)/(N\ P + d)^2 \tag{30}$$

$$E_p = (-F\ L\ N\ \Delta P)/(N\ P + d)^2 \tag{31}$$

$$E_N = (-F\ L\ P\ \Delta N)/(N\ P + d)^2 \tag{32}$$

Tables 14 and 15 list the absolute values of the estimated maximum errors for the camera with 16 mm lens in ALTBIT and NOALTBIT modes. The tables were obtained by substitution of the values listed in Table 16 into Equations (28) through (32). The E_{rss} and $\%E_{rss}$ were calculated by substituting the errors listed in Tables 14 and 15 into Equation (20). Table 17 illustrates the results for the camera with the 16 mm lens in both modes of operation.

The error analysis for the camera with a 50 mm lens was performed by calculating the values of L and then computing the magnitudes of error. Using Equation (25) with values of Hmax, Hmin, P, Nmax, Nmin, listed in Table 16, d and L were found to be equal to 10.36 and 62.93 mm, respectively. Equations (28) through (32) were then used to estimate the maximum errors. Tables 18 and 19 list the absolute values of

TABLE 14

Results of Error Analysis for the Camera with the 16 mm Lens in ALTBIT Mode

H (mm)	N	$\|E_F\|$ (mm)	$\|E_L\|$ (mm)	$\|E_d\|$ (mm)	$\|E_p\|$ (mm)	$\|E_N\|$ (mm)
200.0	125	6.25	0.51	6.35	0.64	0.27
249.8	52	7.81	0.64	9.92	0.40	0.43
300.0	3	9.38	0.76	14.30	0.03	0.61

TABLE 15

Results of Error Analysis for the Camera with the 16 mm Lens in NOALTBIT Mode

H (mm)	N	$\|E_F\|$ (mm)	$\|E_L\|$ (mm)	$\|E_d\|$ (mm)	$\|E_p\|$ (mm)	$\|E_N\|$ (mm)
200.0	250	6.25	0.51	6.35	0.64	0.14
249.8	104	7.81	0.64	9.92	0.40	0.22
300.0	6	9.38	0.76	14.30	0.03	0.31

TABLE 16

Parameters Used in Error Analysis for the Camera with the 16 mm Lens

PARAMETER	NUMERICAL VALUE
L	196.67 mm
F	16.00 mm
d	10.36 mm
P	0.043(0.0215) mm
Nmin	3 (6)
Nmax	125 (250)
Hmin	200 mm
Hmax	300 mm
ΔL	0.5 mm
ΔF	0.5 mm
Δd	0.5 mm
ΔP	0.0004(0.0002) mm
ΔN	0.5

TABLE 17

E_{rss} and $\%E_{rss}$ for the Camera with the 16 mm Lens in Two Modes of Operation

H	E_{rss} ALTBIT	E_{rss} NOALTBIT	$\%E_{rss}$ ALTBIT	$\%E_{rss}$ NOALTBIT
(mm)	(mm)	(mm)		
200.0	8.95	8.95	4.48	4.48
249.8	12.66	12.65	5.07	5.06
300.0	17.13	17.12	5.71	5.71

TABLE 18

Results of Error Analysis for the Camera with the 50 mm Lens in ALTBIT Mode

H (mm)	N	$\|E_F\|$ (mm)	$\|E_L\|$ (mm)	$\|E_d\|$ (mm)	$\|E_p\|$ (mm)	$\|E_N\|$ (mm)
200.0	125	2.00	1.60	6.35	0.64	0.27
249.8	52	2.50	1.98	9.92	0.40	0.4
300.0	3	3.00	2.38	14.30	0.03	0.61

TABLE 19

Results of Error Analysis for the Camera with the 50 mm Lens in NOALTBIT Mode

H (mm)	N	$\|E_F\|$ (mm)	$\|E_L\|$ (mm)	$\|E_d\|$ (mm)	$\|E_p\|$ (mm)	$\|E_N\|$ (mm)
200.0	250	2.00	1.60	6.35	0.64	0.14
249.8	104	2.50	1.98	9.92	0.40	0.21
300.0	6	3.00	2.38	14.30	0.03	0.31

TABLE 20

E_{rss} and $\%E_{rss}$ for the Camera with the 50 mm Lens in Two Modes of Operation

H	E_{rss} ALTBIT	E_{rss} NOALTBIT	$\%E_{rss}$ ALTBIT	$\%E_{rss}$ NOALTBIT
(mm)	(mm)	(mm)		
200.0	6.89	6.88	3.4	3.4
249.8	10.44	10.43	4.2	4.2
300.0	14.82	14.81	4.9	4.9

error in ALTBIT and NOALTBIT modes and Table 20 lists the E_{rss} and $\%E_{rss}$ for both modes.

The results of error analysis listed in Tables 14, 15, 18, and 19 indicate that E_d, E_p, and E_N were the same for both lenses while E_L was smaller and E_F was larger for the 16 mm lens than the 50 mm. The results of E_{rss} and $\%E_{rss}$, listed in Tables 17 and 20, were larger for the 16 mm lens than the 50 mm lens. Therefore, the 50 mm lens was chosen for further analysis.

5.1.3 NOALTBIT vs.ALTBIT Mode

A comparison between Tables 18 and 19 indicated that E_F, E_L, E_d, and E_p were the same in both ALTBIT and NOALTBIT modes while E_N was twice as small in NOALTBIT than ALTBIT mode. Since calibration would considerably reduce the error caused by parameters F, L, and d, NOALTBIT should offer a smaller error due to a smaller E_N.

Although NOALTBIT mode could reduce the error, it would slow down the data collection rate for two reasons. The picture transfered in NOALTBIT mode (128 x 256) was 4 times bigger than that of ALTBIT mode (64 x 128) and additional software was required to rearrange the pixels in a picture taken in NOALTBIT mode to obtain a proper row-to-column ratio for analysis and display. The ALTBIT mode was chosen since it provided a better transfer rate and a more uniform pixel arrangement (Figure 6).

5.1.4 Parallel vs. Slanted RAM-Lens Arrangement

The next option to be examined was installation of the RAM in an angle with the 50 mm lens for formation of more uniformly focused images

on the RAM surface. This option in comparison to the RAM and the lens parallel (Figure 15), was considered an inefficient design because the height measurement model obtained from it was complex. A more complex algorithm would reduce the speed and complicate the calibration procedures.

Other problems with this arrangement were the numerous design options and difficulty in construction of such designs. The new camera was constructed based on the 50 mm lens and the total RAM surface parallel.

5.2 CONSTRUCTION OF THE NEW CAMERA

The new camera was designed and constructed according to the values of parameters d and L calculated from the error analysis of the camera with a 50 mm lens. A steel cylinder with outside and inside diameters of 7.6 and 6.6 cm, respectively, and a height of 5.0 cm was used as the camera case. The top of the cylinder was covered by a circular aluminum plate with a 3.2 cm diameter hole made for insertion of RAM. A 8.9 x 7.0 x 0.7 cm aluminum plate with a 3.2 cm diameter hole for the lens was constructed which was fastened to the base of the cylinder with two screws.

The length of the plate holding the lens was chosen larger than the diameter of the cylinder to offer a range of 0.40 cm to 2.65 cm for the adjustment of parameter d in Figure 15. The distance F could also vary from 5.0 cm to 6.5 cm facilitating the use of lenses with greater than 50 mm focal length and a wider range for focusing the image. This variation was accomplished by unscrewing the lens (enhancing the focal

length of the lens) and sliding the RAM up or down in the top plate hole.

Since the distance between the laser beam and the CLP was 0.6 cm smaller than the radius of the cylinder, the cylinder was cut to provide the appropriate spacing. A 5.0 x 3.8 x 0.5 cm plate, with 2 screw holes to tie the camera to the CLP, was welded to the back of the cylinder. Figure 16 shows the schematic of the new camera.

5.3 CALIBRATION AND DATA ANALYSIS

The new camera was calibrated in a similar manner as the original one. The camera was fastened to the CLP by 2 screws after adjusting the dimensions of F, L, and d for the desirable range of operation (200 to 300 mm). The parameters F, L, and d were measured by caliper and were equal to 55, 47, and 8 mm, respectively. An aluminum sheet with a pin-hole was placed between the metal shutter, which did not shut completely, and the lens to reduce the lens opening (to increase F-Stop) and the amount of light passing through the lens.

The metal stand was raised to hold the profiler 300 mm above the table surface. The distance between the table and the lens was measured with a steel tape at the motor end, the center, and the gear end of the profiler. Then the aluminum block step heights were measured by a caliper and subtracted from the table-to-lens distances measured at 3 different locations along the profiler (MH).

The model used for data collection was Equation (25) with N being replaced by 128-D (ALTBIT mode) and F, L, d, and P with 55, 47, 8, and

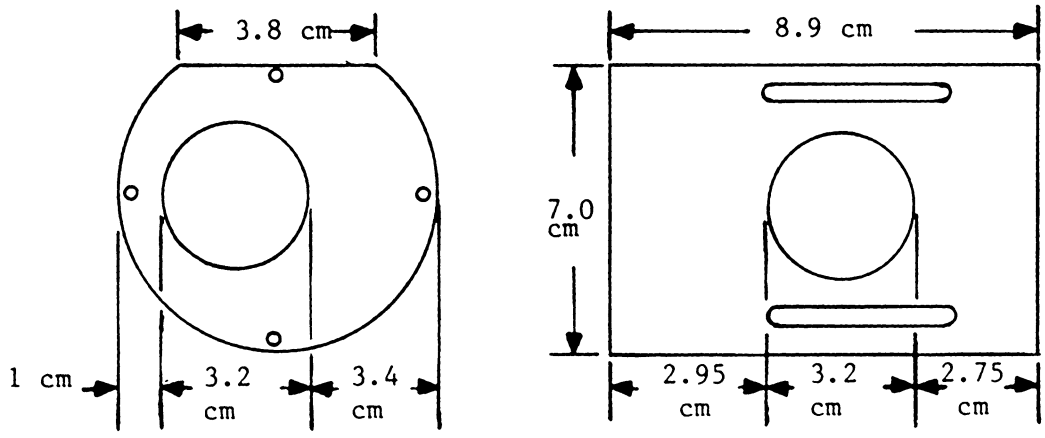

a. Top View
(RAM Plate)

b. Bottom View
(Lens Plate)

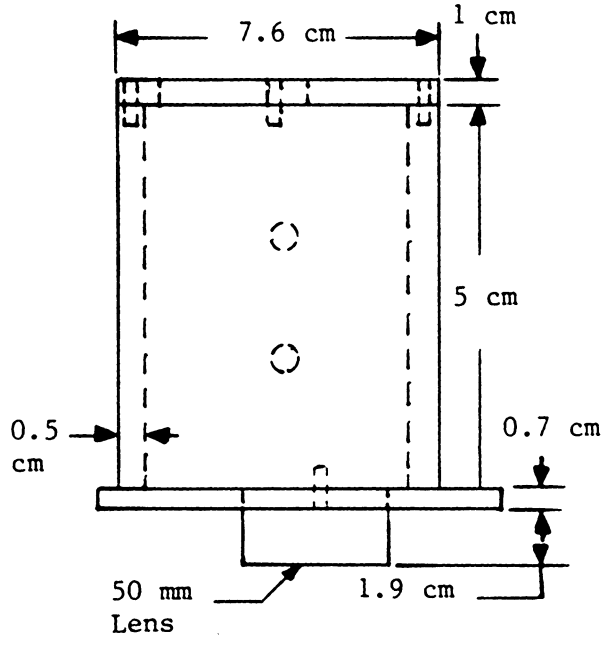

c. Front View

Figure 16. Schematic of the New Camera

0.043 mm. Substitution of the above values for each parameter in Equation (25) resulted in:

$$TH = 6011.6/(314.56 - D) \quad (33)$$

where, TH was the theoretical height (height calculated by the profiler using Equation (33)). Utilizing Equation (33), number of pixels, D, and TH were calcualted and displayed for each target block step (a total of 7 steps), color (black and white), and location (motor end, center, and gear end). The data collection was replciated 5 times. The data are shown in Appendix F.

The calibration data were statistically analyzed to develop a model, similar to Equation (25), and to investigate the effect of surface color, and the horizontal position of the CLP (rod deflection) on the calculation of the height. The data were organized in terms of color and position (motor end, center, and gear end) and two non-linear models were fit to each set for analysis.

The two models were:

$$MH = k_1/(k_2 - D) + e \quad (34)$$

and:

$$MH = k_1/(k_2 - D) + k_3 + e \quad (35)$$

where:

MH - measured height (known)

D - number of pixels (known)

k_1, k_2, k_3 - unknown constants

e - random error.

The constants k_1 and k_2 in Equations (34) and (35) were unknown constants representing FL/P and 128 + d/P. The unknown constant, k_3,

was added to the second model in order to account for the uncertainty in measuring MH and difficulty of knowing the exact location of the focal point.

Table 21 lists the residual mean square (RMS) for each set of data using each model. The RMS listed in Table 21 indicated a difference between the two models. Therefore, the two models, using all the data, were compared and Equation (35) with k_1, k_2, and k_3 equal to 7370.0, 338.9, and -2.75 was chosen because it resulted in a significantly smaller RMS (.0011 cm^2). Appendix G shows the program used for the statistical analysis of the data collected for calibration of the new camera.

5.4 TESTING THE NEW CAMERA WITH ACTUAL SOIL

The second model, Equation (35) obtained from calibration of the new camera, was tested with actual soil. Five soil samples, varying in color from very light to fairly dark, were used. Four of the soil samples were used both dry and wet to produce a wider range of colors and one sample was mixed with oil which offered flexiblity in forming the soil into different geometries. Table 22 describes the color of each of the soil samples. The table was obtained by comparing the samples with the Reference Munsell Soil Color Charts.

A 150.0 x 1.9 x 1.4 cm U-shape aluminum tube was used as the soil sample container. The soil samples were first seived then the tube was filled with the soil and the surface was slightly compacted to provide a flat surface the same level as the tube rim. The tube containing the soil sample was then placed under the profiler. The distance between the lens and the soil surface was adjusted to be equal to Hmin (200

TABLE 21

A Comparison Between Residual Mean Squares (RMS) of Model 1 (Equation (34)) and Model 2 (Equation (35)) using the Camera with the 50 mm Lens

COLOR	POSITION							MODEL
	1	2	3	1&2	1&3	2&3	1&2&3	
BLACK	.0009	.0014	.0012	.0018	.0026	.0014	.0022	1
WHITE	.0010	.0010	.0009	.0015	.0023	.0010	.0018	1
B&W	.0010	.0012	.0010	.0017	.0024	.0013	.0020	1
BLACK	.0001	.0004	.0002	.0009	.0017	.0004	.0012	2
WHITE	.0001	.0001	.0002	.0006	.0014	.0003	.0010	2
B&W	.0001	.0003	.0002	.0008	.0015	.0004	.0011	2

TABLE 22

Colors of Soil Samples

SOIL NUMBER	SOIL CONDITION	SOIL COLOR
1	OILY	DARK GRAY
2	DRY	GRAYISH BROWN
3	WET	VERY DARK GRAYISH BROWN
4	DRY	REDDISH YELLOW
5	WET	STRONG BROWN
6	DRY	VERY PALE BROWN
7	WET	DARK YELLOWISH BROWN
8	DRY	YELLOW
9	WET	YELLOWISH BROWN

mm). At LEVEL 1 (Hmin) 43 theoretical heights (TH1), in 3 cm horizontal intervals, were calculated using Equation (35). The data collection was carried out 3 times. The distance between the lens and the soil surface was measured by a steel tape at the two ends of the profiler (MH1). The intermediate heights, in 3 cm intervals, were computed using the equation of a straight line with the known coordinates being the heights and horizontal distances at the motor and the gear ends.

The profiler was raised 5 cm at both ends (LEVEL 2). The change in height was measured with a caliper and was added to the initial heights, MH1, measured at the motor and the gear ends (MH2). The new intermediate heights were computed using the new coordinates. The theoretical heights (TH2), in horizontal increments of 3 cm were measured 3 different times using Equation (35). The same procedure was carried out for the profiler at a 300 mm distance above the soil surface (LEVEL 3).

The height calculations were repeated for each of the 9 soil samples. The data were then analyzed to investigate the effect of soil color, rod deflection (the CLP horizontal travel), and the veritcal distance between the lens and the soil surface on the height measurements, to find the error and to test the validity of Equation (35). Appendix H shows the list of the data collected from the 9 soil samples.

5.5 ANALYSIS OF THE ACTUAL SOIL DATA

The data analysis was performed two different ways. In the first analysis, the difference in heights measured by the steel tape and calculated by profiler (DIF1 = MHn - THn, where n was level 1, 2, or 3) were used. In the second analysis the difference in levels (DIF2 = (MH2 - MHn) - (TH2 - THn), where n was either 1 or 3) were used rather than

the absolute heights, since the change in the soil heights was the subject of investigation in erosion studies.

An analysis of variance (ANOVA) was performed on the data using model:

$$MHn - THn = C + R + V + CR + CV + RV + CRV + e \qquad (36)$$

where:

MHn - THn - difference between measured and theoretical heights (DIF1)

C - color effect (a total of 9 colors)

R - rod deflection (horizontal displacement) effect (5 points out of a total of 43 points)

V - level (vertical distance) effect (3 levels)

e - random error.

The ANOVA was performed to determine the effect of each factor (C, R, and V) and each interaction (CR,...) on the difference of heights (DIF1). The results obtained from ANOVA indicated that all factors had an effect on the difference in heights (all the effects were significant at 0.05 level).

In order to detect the effect of individual factors a Duncan's multiple range test (DMRT) was required. The DMRT is utilized when a comparison among the means of nonindependent treatments is required. This method compares each mean with every other mean by ranking the means from smallest to largest. The results of DMRT are summarized in Table 23 and the means, standard deviations, and standard error of means for DIF1 at all 3 levels are listed in Table 24.

A similar ANOVA was required to determine the effect of color, level, and deflection on the difference between the measured and the theoretical change in heights (DIF2) with respect to LEVEL 2. The model used was:

$$(MH2 - MHn) - (TH2 - THn) = C + R + V + CR + CV + RV + CRV + e \quad (37)$$

where:

MH2 and TH2 - measured and theoretical heights of LEVEL 2

MHn and THn - measured and theoretical heights of LEVEL 1 and LEVEL 3.

The results of ANOVA indicated that all effects (C, R, and V) and all interactions (CR, CV, etc.) were statistically significant at 0.05 level, therefore a DMRT was required to detect the effect of individual factors on heights difference (DIF2). Table 25 shows the results of the DMRT and Table 26 lists the means, standard deviations, and standard error of means of the data using the model DIF2.

TABLE 23

Results of DMRT Using Model DIF1

SOIL COLOR	MEAN (cm)	GROUPING			
1	0.154	A			
4	0.133	A	B		
7	0.131	A	B	C	
3	0.121	A	B	C	
6	0.116	A	B	C	
5	0.109	A	B	C	
2	0.087		B	C	
8	0.069			C	D
9	0.027				D

TABLE 24

Means, Standard Deviations and Standard Error of Means for the Data at Levels 1, 2, and 3 Using Model DIF1

LEVEL	MEAN (cm)	STANDARD DEVIATION (cm)	STD. ERROR OF MEAN (cm)
1	0.095	0.094	0.008
2	0.110	0.092	0.008
3	0.111	0.092	0.008

TABLE 25

Results of DMRT Using Model DIF2

SOIL COLOR	MEAN (cm)	GROUPING		
9	0.040	A		
1	0.024	A	B	
7	0.024	A	B	
2	0.023	A	B	
3	0.008	A	B	
8	0.007	A	B	
4	0.001	A	B	
5	-0.006		B	
6	-0.056			C

TABLE 26

Means, Standard Deviations, and Standard Error of Means for the Data at L2 - L1 and L3 - L2 Using Model DIF2

LEVEL	MEAN (cm)	STANDARD DEVIATION (cm)	STD. ERROR OF MEAN (cm)
L2 - L1	0.015	0.037	0.0031
L3 - L2	-0.001	0.041	0.0035

5.6 PROFILER PERFORMANCE IN THE SUN LIGHT

Since future use of the profiler depends on how well it performs in the field, the profiler was evaluated outside the laboratory (in sunlight). This evaluation was particularly important because the wavelength of the laser beam (623 nm) was within the 400 to 700 nm range of sunlight.

The device was set under sunlight and the pictures of the laser beam were taken and displayed. To take an acceptable picture, the exposure time needed to be shortened based on light intensity through the software. After adjusting the exposure time, the laser beam could be distinguished from the sunlight by the camera and surface heights could be computed for each picture. Since the objective of this research was to utilize the profiler under the laboratory conditions, no attempt was made to calibrate the device for outdoor conditions.

5.7 THE NEW DESIGN DISCUSSION

Design of a new camera was necessary for reduction in the height measurement error. Several options were analyzed and the errors, obtained from error analysis, were compared to design a more accurate camera. The first option was the use of the whole surface area of the RAM which reduced the error by improving the resolution and doubling N in the denominator of the error terms (Equations (16) through (19)).

The next option was to compare the 16 mm lens with a 50 mm lens, utilizing the whole surface area of the RAM in both cases. Results of error analysis listed in Tables 14 and 15, for the 16 mm lens, and 18 and 19, for the 50 mm lens, indicated that E_d, E_p, and E_N were the same

for both lenses in each operation mode, but E_F and E_L were about 3 times smaller for the 50 mm lens than the 16 mm one. Comparison of E_{rss} and $\%E_{rss}$, listed in Tables 17 and 20, showed that they were larger for the 16 mm, which was expected due to larger E_L and E_F. The 50 mm lens was chosen since it offered smaller uncalibrated errors and a smaller L.

The third option was to reduce the error caused by the unfocused image by installing the RAM in an angle with the 50 mm lens. The choice of an angle from a large number of angles, the complexity of the model affecting the speed and complicating the calbiration procedure, and difficulty in construction of such a design were the reasons for using the design depicted in Figure 15.

The last option to be examined was NOALTBIT vs. ALTBIT mode. Results of error, listed in Tables 17 and 18, indicated that except E_N, which was twice as big for ALTBIT than NOALTBIT mode, E_F, E_L, E_d, and E_p were the same. Results of E_{rss} and $\%E_{rss}$, listed in Table 20 for both modes of operation, were the same (uncalibrated error) which would become smaller for NOALTBIT mode after calibration reducing E_F, E_L, and E_d.

The NOALTBIT mode would offer a better accuracy than ALTBIT mode, it would also reduce the speed of data collection considerably (about 4 times) and therefore was not used. The speed reduction is due to transmission of a bigger picture and development of a program to produce a picture with the proper row-to-column ratio by rearranging the pixels.

The new camera was built based on Figure 15, utilizing a 50 mm lens and the whole surface area of the RAM. The profiler was calibrated by operating the camera in ALTBIT mode. The model developed (Equation

(35)) produced a calibrated error of ±0.68 mm. Figure 17 illustrates a plot of residual vs. measured height for the models.

The accuracy of model 2 was tested by collecting data from 9 different soil samples at 200, 250, and 300 mm levels. The analysis of variance (ANOVA) for both DIF1 and DIF2 models showed that all factors (color, position, and level) had a significant effect on the height measurements.

The results of Duncan's multiple range test (DMRT) for DIF1, listed in Table 23, indicated that the mean of soil number 9 (yellowish brown) was different than the rest but soil number 8 (yellow), and mean of soil number 1 (dark gray) was different than 2 (grayish brown). Since the means of darker and brighter colors (very dark grayish brown, soil number 3, and very pale brown, soil number 6) were not different, the differences due to soil color 9 and 1 could have been the result of uneven surface due to particle sizes.

The error at each level (1, 2, and 3) was computed by multiplying the standard error of mean by 1.64 (for the normal, z, distribution at 0.95 level) and adding it to the mean (Table 24). The errors were equal to 1.08, 1.20, 1.20 mm in levels 1, 2, and 3, respectively. One reason for having errors greater than the calibration error (±0.68 mm) was the fact that DIF1 included the rod deflection effect on difference in height (THn - MHn), since it used the theoretical height (straight rods) rather than the actual height (deflected rods). Another reason was that the surface of the soil samples could not be as flat as the surface of the calibration block. The slight difference in error between levels was expected as shown by the error analysis and as seen in Figure 17.

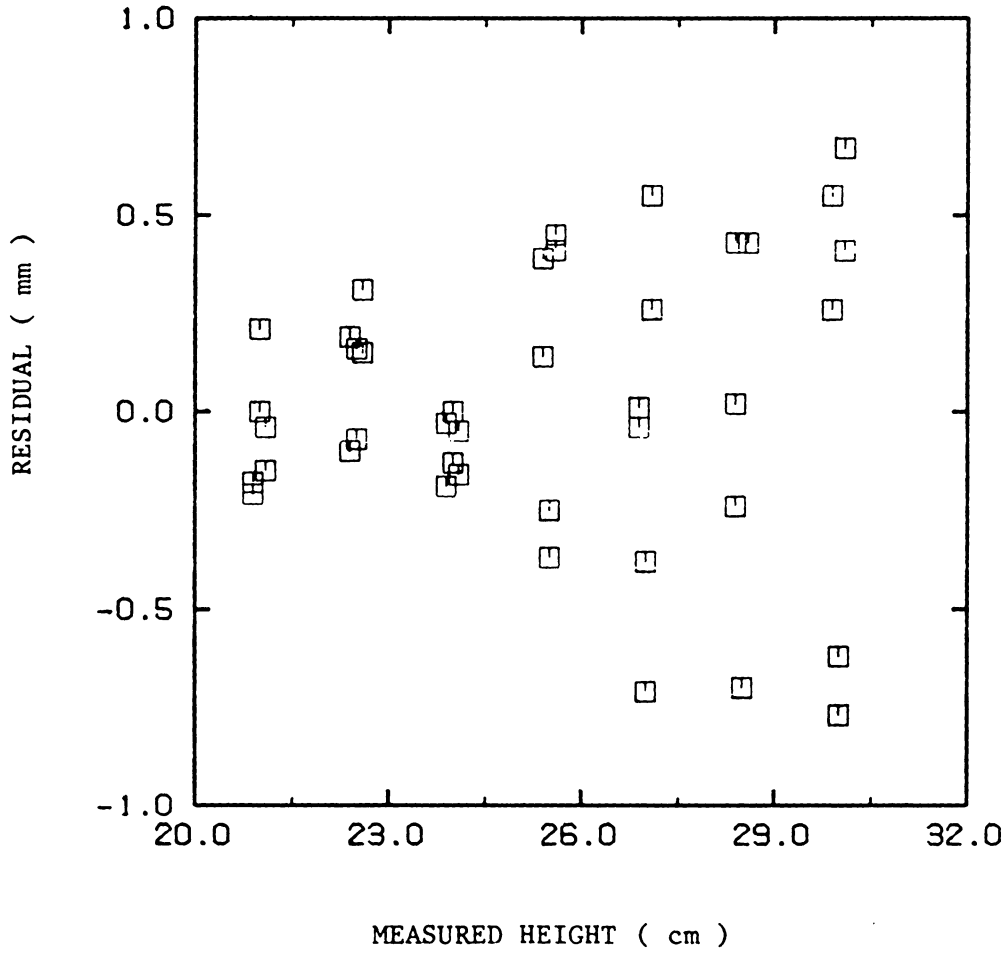

Figure 17. Residual vs. Measured Height
for Equation (35)

The results of DMRT for model DIF2, listed in Table 24, indicated that the mean of color 6 (very pale brown) was different than the rest, and the mean of color 9 (yellowish brown) was different than that of color 5 (strong brown). The difference between colors could have resulted from the particle sizes or the surface of the samples.

The error at each level (L2 - L1 and L3 - L2) was computed by multiplying the standard error of mean by 1.64 and adding it to the mean (Table 26). The results were .20 mm at L2 - L1 and 0.07 mm at L3 - L2. These errors were smaller than the errors obtained from calibration and from model DIF1, since model DIF2 eliminated the rod deflection effect on error (which was included in DIF1) and computed the error for the difference instead of absolute heights (which was performed in calibration).

Chapter VI

SUMMARY AND CONCLUSIONS

A mechanical, non-contact soil profile meter was designed and constructed to study the erosion caused by the artificial rainfall under laboratory conditions. The design goal was to measure the surface heights of a 1.5 x 1.5 m soil bin with an accuracy of 1.0 mm at a rate of 2 points per second.

The profiler consisted of a height measuring unit, a horizontal drive system, a control unit, and a data processing unit. The height measuring unit utilized a digital camera and a laser. The camera consisted of a 16 mm lens and an Optic random access memory (Optic RAM of the dynamic type) made of 256 x 256 array of light sensitive capacitors (pixels). The laser was used for reliabiltiy in operation and production of a highly intense, very uniform, and narrow beam (0.63 mm in diameter).

The horizontal drive system consisted of a stepper motor, a plastic-coated steel chain, 2 steel rods, gears and linear ball bearings. The stepper motor was used for ease in interface and control, precision, and controllable speed and grid size.

The electronics to control the motor and the camera, and the microcomputer to process the data made up the control system and the data processing unit.

The principle of height measurement was based on similar triangles. A laser beam struck the surface of the soil and the reflection was focused by the lens on the RAM surface discharging a number of pixels toward zero volts. The distance between the discharged pixels

and a reference point on the RAM (NP) varied in a non-linear and inverse relationship with the distance between the lens and the surface (H). The height H for each point was calculated by computing NP through a search-and-count routine and measuring the lens-to-RAM (F) and the camera-to-laser (L) distances (both of which were fixed).

The height measuring unit was calibrated by collecting data from a 7-step aluminum block covered with a black and a white tape at 3 locations along the profiler. The calibration was performed to determine the effect of color, position (rod deflection), and vertical distance on the height measurements. It was also used to develop a model with a small error. The error was 1.95 mm for the camera with the 16 mm lens, utilizing half of the RAM surface, and operating in the ALTBIT mode (using even-numbered pixels and rows).

A new camera was designed from several options, based upon error analysis, to improve the height measurement accuracy. The new design utilized the whole RAM surface and a 50 mm lens. The height measuring unit was calibrated and the new model was tested with the real soil samples. The horizontal drive system was also calibrated to determine the repeatability and positioning accuracy of the profiler. The overall performance of the profiler and the calibration results are listed below.

1. The accuracy of the drive system was ±0.12 mm which was smaller than the laser beam diameter (0.63 mm).
2. The calibrated accuracy of the new height measuring unit was ±0.68 mm for the camera in ALTBIT mode of operation.
3. The rate of data collection was 32 points per minute.

4. The analysis of the data collected from the 9 different soil samples indicated that color, rod deflection, and vertical distance between the lens and the surface were all significant at 0.05 level and, therefore, all of the variables affected the height measurements.
5. The error associated with the absolute heights of the soil samples, including the effect of rod deflection, was 1.2 mm and the error for the difference in heights was 0.2 mm.
6. The outdoor performance of the profiler was tested under sunlight and was satisfactory. However, the exposure time needed to vary to compensate for the variation in the intensity of natural light.

The soil profiler developed for the erosion studies could also be used in other applications requiring soil profile measurement. A few examples are tillage evaluation, seedbed preparation, surface water storage, and off-road vehicle performance studies. It has the advantages of the mechanical, non-contact profilers such as, no interference with the soil surface, capability of collecting and manipulating a large number of data points, and variable grid size. It also offers a great deal of flexibility and versatility via software and leads to a whole new range of applications (i.e., plant growth detection, lumber deflection measurement, leaf area calculation, etc.).

Chapter VIII

SUGGESTIONS FOR FURTHER RESEARCH

The existing height measurement error of ±0.68 mm could be reduced by using the camera in NOALTBIT mode and including variables in the height measuring model to account for the change in color (from a reference color), rod deflection, and vertical distance between the camera and the surface. Although accuracy can be improved by the above methods, the speed of operation would also be reduced since the picture size quadruples and the software would be more complex.

From Table 2 the transmission time of a 64 x 19 picture at a baud rate of 9600 bps is 1267 ms which results in a total transmission time of 40 seconds for 32 points (pictures). It takes the motor 1125 msec to move the CLP from one point to the next (3 cm increments). Since the data can be transferred and manipulated while the motor runs and the data transfer rate (1267 ms per picture) is larger than the 1125 ms travel time of motor between 2 points, the motor speed does not affect the rate of data collection and the remaining 20 seconds is the time used by the software.

The speed of data collection could be improved by increasing the baud rate (since 2/3 of the time is taken by transfer of data) by writing portions of the software in assembly language. It could be further improved by transferring and searching only the rows of picture that contain the laser image. A faster motor is required if the data transfer time gets smaller than 1125 ms.

The rod deflection does not affect the height measurements in applications where the difference in height is to be measured (i.e.,

erosion studies) because rod deflection is repeated in measurements before and after a rainfall event and therefore can be eliminated by subtraction of the two measurements. In applications that require the measurement of absolute heights a model could be developed which would include a variable term to correct for the deflection.

There are several ways to solve the problem of adjusting the exposure time under the outdoor conditions. One way is to use an optical filter to only allow the laser frequency into the camera (reject all the wavelengths except 623 nm ±10 nm). Another solution is to measure the light intensity through hardware and adjust the exposure time accordingly via software. The last and the least expensive solution is to block the sunlight by a shade.

LITERATURE CITED

Burwell, R. E., R. R. Allmaras, and M. Amemiya. 1963. A field measurement of total porosity and surface microrelief of soils. Soil Sci. Soc. Amer. proc. 27(6):697-700.

Ciarcia, S. A. 1983. A 64K-bit dynamic RAM chip is the visual sensor in this digital image camera. BYTE, 8(9):21-31.

Currence, H. D. and W. G. Lovely. 1970. The analysis of soil surface roughness. Transactions of ASAE, 13(6):710-714.

Currence, H. D., and W. G. Lovely. 1971. An automatic soil surface profilemetre. Transactions of ASAE, 14(1):69-71.

Curtis, W. R., and W. D. Cole. 1972. Micro-topographic profile gage. Agricultural Engineering, 53(1):17.

Dexter, A. R. 1977. Effect of rainfall on the surface micro-relief of tilled soil. J. of Terramechanics 14(1):11-22.

Doebelin, E. O. 1983. Measurement systems application and design, McGraw-Hill, Inc., pp. 58-67.

Ealing Corporation. 1984. Ealing Optics Catalog. Harvard Bioscience. Massachusetts.

Harral, B. B., and C. A. Cove. 1982. Development of an optical displacement transducer for the measurement of soil surface profiles. Journal of Agricultural Engineering Research, 27:421-429.

Heerman, D. F., R. J. Wenstrom and N. A. Evans. 1969. Prediction of flow resistance in furrows from soil roughness. Transactions of the ASME 12(4):482-485,489.

Henry, J. E., M. J. Sciarini, and D. M. Van Doren, Jr. 1980. A device for measuring soil surface profiles. Transactions of ASAE, 23(6):1457-1459.

Hirschi, M. C., B. J. Barfield, and I. D. Moore. 1984. Rillmeters for detailed measurement of soil surface heights. ASAE paper no. 84-2534.

Johnson, C. W., and J. P. Smith. 1983. Soil loss caused by off-road vehicle use on steep slopes. Transactions of the ASAE 26(2):402-405.

Kuipers, H. 1957. A relief meter for soil cultivation studies. Neth. J. Agric. Sci. 5:255-262.

Kuipers, H., and C. Van Ouwerkerk. 1963. Total pore-space estimation in freshly ploughed soil. Neth. J. Agric. Sci. 11:45.

Merva, G. E., R. D. Brazee, G. D. Schwab and R. B. Curry. 1970. Thoeretical considerations of watershed surface description. Transactions of the ASAE. 13(14):462-465.

Micromint, Inc. 1983. Micro D-Cam Apple Version, Users Manual. 561 Willow Avenue, Cedarhurst, NY, 11516.

Mitchell, J. K., and B. A. Jones, Jr. 1973. Profile measuring device. Transactions of ASAE, 16(3):546-547.

Mitchell, J. K., and B. A. Jones. 1976. Micro-relief surface depression storage: Analysis of models to describe thedepth-storage function. Water Res. Bull. 12(6):1205-1222.

Mitchell, J. K., and B. A. Jones. 1978. Micro-relief surface depression storage: charges during rainfall events and their application to rainfall-runoff models. Water Res. Bull. 14(4):777-802.

Molnau, M., En Shang Yen, and L. A. Druffel. 1984. Overwinter random roughness changes for four tillage practices. ASAE paper no. 84-2506.

Moore, J. D., and C. L. Larson. 1979. Estimating microreflief surface storage from point data. Transaction of ASAE, 22(5):1073-1077.

Podmore, T. H., and L. F. Huggins. 1981. An automated profile meter. American Society of Agricultural Engieers. Paper no. 82-2620.

Radke, J. K., M. A. Otterby, R. A. Young and C. A. Onstad. 1981. A microprocessor automated rillmeter. Transactions of ASAE, 24(2):401-404.

Riley, S. J. 1983. An inexpensive gage for measuring ground surface topography. Transactions of the ASAE 26(3):831-832.

Rogers Labs, Inc. 1984. A6 T/D Timer Driver board for the Apple II/IIe Comter user's manual. California.

Rogoski, Khanbilvardi, and Jones. 1984. Point estimates of erosion. ASAE paper no. 84-2035.

Romkens, M. J. M, S. Singarayar, and C. J. Gantzer. 1982. An automated noncontact surface profile meter. American Society of Agricultural Engineers. Paper no. 82-2620.

Romkens, M. J. M., and J. Y. Wang. 1985. Soil roughness changes of tillage systems from rainfall. ASAE paper No. 85-2048, ASAE, St. Joseph, MI 49085.

Schafer, R. L., and W. G. Lovely. 1967. A recording soil surface profile meter. Agricultural Engineering 48:280-282.

Van Ouwerkerk, C. M. Pot, and K. Boersma. 1982. Electronic mocro-reliefmeter for seedbed characterization. Soil and tillage research, 2:81-90.

Wilton, B. 1964. Effect of cultivations on the level of the surface of a soil. J. Agric. Engng. Res. 9:214.

Winfred M. Berg, Inc. The complete manual of precision mechanical components, New York.

Appendix A

Camera Control Software

```
Variable LTM 5000 LTM !
: ACIA   3 49406 C! 20 49406 C! ;
: GR     49235 C@ 49239 C@ 49236 C@ 49232 C@ ;
: CHK1   BEGIN 49406 C@ 2 AND 0) UNTIL ;
: CLEAR  16383 8192 DO 0 I C! LOOP ;
: SOKNS  CHK1 211 49407 C! ;
: REFNS  CHK1 209 49407 C! ;
: REFS   CHK1 208 49407 C! ;
: WAIT   LTM @ 0 DO LOOP ;
: SET    CLEAR GR ;
: C@SC!  [ 1, LDY, 0; STY, 0; LDA9X 1, STA, 1, LDA, 2, LDY, 1;
         STY, 1; STA9X INX INX RTS
: NRUN   8192 8 0 DO DUP I 128 * + 8 0 DO DUP I 1024 * + 19 0 DO
         DUP I + BEGIN 49406 C@ 1 AND 0) UNTIL 49407 C@SC! LOOP
         DROP LOOP DROP LOOP DROP ;
: GET    ACIA SOKNS WAIT REFS NRUN REFNS ;
```

FORTH DEFINITION	FUNCTION
ACIA	Resets the ACIA and specifies the transit protocol by writing a 3 and a 20 decimal to address 49406 (status register).
GR	Sets the monitor to first page of high resolution graphics mixed with text.
CHK1	Checks to see when the camera can receive a command byte by reading the status register (camera is ready when bit1 of the content of address 49407 is 1).
CLEAR	Clears the first graphics page.
SOKNS	Writes 211 into data register, when CHK1 is true, to allow the pixels to discharge for a specific exposure time (SOAK) without transmitting a picture to the computer (NOSEND).
REFNS	Writes 209 into data register (address 49407) to allow the pixels to charge up (REFRESH) without sending the picture to computer (NOSEND).
REFS	Writes 208 into data register to REFRESH and SEND the data to the computer when CHK1 is true.
WAIT	Uses the variable LTM to provide the specified exposure time.
SET	Clears and sets the screen.
C@SC!	Reads the data from the camera and writes it on screen (it is coded in FORTH assembly).

NRUN — Sets the screen addresses (the starting address of page 1 is 8192 which is incremented by 1024 every 8 rows and by 128 every row), checks the camera to find out when the data are transmitted (bit0 of status register equal 1), reads the data and writes it on the screen.

GET — Puts all the necessary command together in order to get a picture.

The picture size is 128 x 64 which is obtained by operating the camera in ALTBIT, NOWIDPIX, 1ARRAY, and 7BIT modes. The exposure time is controlled by LTM by writing a number (i.e., n LTM !). To run the software the following command must be executed; 17 LOAD 26 LOAD SET GET where, pages 17 and 26 store the FORTH assembly and the software and SET and GET commands set the screen and get a picture.

Appendix B

Stepper Motor Control Software

```
VARIABLE CBAS 49312 CBAS !

VARIABLE SPEED 150 SPEED !

VARIABLE LAT 49900 LAT !

: OTPT   CBAS @ + C! ;

: STCT3  0 1 OTPT 131 0 OTPT ;

: STCT2 160 1 OTPT ;

: CNT3   SPEED @ 255 /MOD 6 OTPT 7 OTPT ;

: CNT2   255 /MOD 4 OTPT 5 OTPT ;

: STCNT  161 1 OTPT 0 0 OTPT ;

: BACK   2 LAT @ C! ;

: FORE   3 LAT @ C! ;

: STSP   SPEED ! ;

: STSTEP STCT3 STCT2 ;

: START  STSTEP 400 STSP CNT3 STCNT ;

: START  START 0 CNT2 ;

: STEPS  CNT2 ;

: CHSPD  STSP CNT3 ;
```

VARIABLE	FUNCTION
CBAS	Contains the base counter address for slot #2 (49312 decimal) where the A6 T/D board is plugged into the microcomputer
SPEED	contains a number corresponding to the speed of stepper motor
LAT	Holds the latch address 49900 decimal

FORTH DEFINITION	FUNCTION
OTPT	Stores the data into base address (49312 decimal)
STCT3	Points to control register #3 by putting a 0 into the address CBAS + 1 and puts a 131 decimal (10000011 binary) into CBAS to: Enable output of Timer #3 (bit7 = 1) Inhabit interrupt when counting through 0 (bit6 = 0) Operate in continuous mode (bit5 = 0) Initialize on register write (bit4 = 0) Operate in continuous mode (bit3 = 0) Use 16 bits for counting (bit2 = 0) Enable (internal) clock used for input (bit1 = 1) Prescale by dividing by 8 (bit0 = 1)

STCT2	Puts a 160 decimal (10100000 binary) into CBAS + 1 (point to register #2) to : Enable the output of Timer #2 (bit7 = 1) Mask interrupt flag on IRQ (bit6 = 0) Operate in single shot mode, write to latch or reset (bit5 = 1, bit4 = 0, bit3 = 0) Count in 16-bit mode (bit2 = 0) Use external clock on $\overline{C2}$ input (bit1 = 0) Write into counter #3 (bit0 = 0)
CNT3	Divides the SPEED by 255 and puts the result in the MSB and LSB of Timer #3
CNT2	Divides any number by 255 and puts the result in the MSB and LSB of Timer #2
STCNT	Puts 161 decimal (101000001 binary) into CBAS + 1 as done by STCT2, except that counter #1 is written into (bit0 = 1). It also starts the counters
FORE	Runs the motor clockwise
BACK	Runs the motor counter-clockwise
STSP	Puts a number into variable SPEED
STSTEP	Executes commands STCT3 and STCT2
START	Initializes the counters, sets the speed to 400, and starts the counters
STEPS	Specifies the number of motor steps
CHSPD	Changes the motor SPEED.

The software is stored in page 49 which can be run by the command 49 LOAD. The A6 T/D board is plugged into slot #2 (CBAS = 49312). The motor could be turned on by the command START BACK/FORE n STEPS

where:

START - used only the first time or when RESET key is pressed

BACK/FORE - direction specifiers

n STEPS - no. of motor steps.

The speed of motor is a variable which can be controlled by SPEED. The command n CHSPD is used to change the speed where n is a number bigger than 150 (speed increases as n gets smaller).

APPENDIX C

Height Measurement Software

```
VARIABLE BITCNT   VARIABLE TOTBIT
VARIABLE BYTES    VARIABLE BYTCNT
VARIABLE TERM
: IN1 0 TOTBIT ! 0 TERM ! ;
: IN2 0 BYTCNT ! 0 BITCNT ! ;
: DOT 8 1 DO 2 /MOD SWAP IF 1 BITCNT +! BYTCNT @ I + TERM +! THEN
      LOOP DROP;
: CNT BYTES @ BYTCNT @ - BITCNT @ * TERM +! ;
: NM  K3 K1 K2 TERM @ ?DROP IF FLOAT TOTBIT @ FLOAT F/ .5 F- 2DUP
      ." N =" F. F- F/ F+ ."  H =" F. ELSE BELL ." GET ANOTHER
      PICTURE" 2DUP 2DROP THEN ;
: AVG IN1 8191 7 0 DO DUP I 128 * + 8 0 DO IN2 DUP I 1024 * + 19
      1 DO DUP I + C@ 127 AND ?DUP IF DOT I 7 * BYTES ! 7 BUTCNT
      +! THEN LOOP DROP BITCNT @ TOTBIT +! CNT LOOP DROP LOOP
      DROP NM ;
```

VARIABLE	FUNCTION
BITCNT	Counts the number of light pixels in a row.
BYTCNT	counts the number of bytes containing light pixels in a row multiplied by 7 (bits per byte).
TOTBIT	Counts the total number of light pixels in a picture.
BYTES	Counts the number of bytes from left up to and including the last byte containing the light pixels in a row multiplied by 7 to convert bytes to bits (BUTES = NOBYTE + BYTCNT).
TERM	Contains the cumulative sum as shown by Equations (14) and (15).

FORTH DEFINITION	FUNCTION
IN1, IN2	Initialize the counters (variables)
DOT	Manipulates a byte containing light pixels to find the SUM and the BITCNT
CNT	Computes the TERM for each row
NM	Uses Equation (15) in conjunction with calibration modesl for 16 or 50 mm lenses to compute N and H (K1, K2, and K3 take the values obtained by calibration models).
AVG	Sets up the screen addresses, gets a byte from the screen and calls the DOT if the byte contains light pixels, otherwise scans through the remaining bytes, and finally calls NM to calculate N and H (cm).

The picture size is 128 x 64 (ALTBIT mode). To run the program the commands 50 LOAD 48 LOAD and AVG should be executed.

Appendix D

Height Measurement Calibration Data Collected by the Camera with the 16 mm Lens

			BLACK TAPE		WHITE TAPE	
TRIAL	POSITION	MH (cm)	D	TH (cm)	D	TH (cm)
1	1	25.90	34.52	26.51	34.64	26.61
		24.40	32.34	24.68	32.67	24.94
		22.91	30.37	23.24	30.39	23.25
		21.41	28.03	21.72	27.44	21.37
		19.90	24.79	19.93	35.06	20.07
		18.40	21.46	18.37	21.53	18.40
		16.92	17.46	16.79	17.43	16.78
1	2	25.79	34.38	26.38	34.32	26.33
		24.28	32.29	24.64	32.08	24.48
		22.79	30.11	23.06	30.02	23.00
		21.29	28.01	21.71	27.41	21.36
		19.78	24.44	19.75	24.53	19.80
		18.28	21.28	18.29	21.20	18.26
		16.80	17.31	16.74	17.10	16.66
1	3	25.90	34.42	26.42	34.40	26.40
		24.40	32.32	24.67	32.36	24.70
		22.91	30.37	23.24	30.05	23.02
		21.41	27.96	21.68	27.29	21.29
		19.90	24.58	19.82	24.88	19.97
		18.40	21.43	18.36	21.41	18.35
		16.92	17.41	16.77	17.44	16.78

			BLACK TAPE		WHITE TAPE	
TRIAL	POSITION	MH (cm)	D	TH (cm)	D	TH (cm)
2	1	25.90	34.54	26.52	34.74	26.71
		24.40	32.31	24.66	32.64	24.92
		22.91	30.37	23.24	30.36	23.23
		21.41	27.98	21.69	27.35	21.32
		19.90	24.68	19.87	25.02	20.05
		18.40	21.48	18.38	21.51	18.39
		16.92	1750	16.80	17.47	16.79
2	2	25.79	34.41	26.41	34.34	26.35
		24.28	32.30	24.65	32.07	24.47
		22.79	30.11	23.06	30.04	23.01
		21.29	27.99	21.70	27.40	21.35
		19.78	24.44	19.75	24.50	19.78
		18.28	21.20	18.26	21.22	18.27
		16.80	17.35	16.75	17.06	16.65
2	3	25.90	34.48	26.47	34.44	26.43
		24.40	32.30	24.65	32.19	24.56
		22.91	30.30	23.19	30.05	23.02
		21.41	27.99	21.70	27.42	21.36
		19.90	24.61	19.84	24.88	19.97
		18.40	21.45	18.36	21.41	18.35
		16.92	17.41	16.77	17.43	16.78

			BLACK TAPE		WHITE TAPE	
TRIAL	POSITION	MH (cm)	D	TH (cm)	D	TH (cm)
3	1	25.90	34.42	26.42	34.63	26.61
		24.40	32.27	24.63	32.64	24.92
		22.91	30.19	23.11	30.35	23.22
		21.41	27.85	21.62	27.36	21.33
		19.90	24.44	19.75	25.04	20.06
		18.40	21.30	18.30	21.48	13.38
		16.92	17.31	16.74	17.44	16.78
3	2	25.79	34.34	26.35	34.39	26.39
		24.28	32.30	24.65	32.17	24.55
		22.79	30.19	23.11	30.01	22.99
		21.29	27.98	21.69	27.34	21.31
		19.78	24.44	19.75	24.46	19.76
		18.28	21.22	18.27	21.21	18.26
		16.80	17.29	16.73	17.07	16.65
3	3	25.90	34.44	26.43	34.45	26.44
		24.40	32.32	24.67	32.24	24.60
		22.91	30.37	23.24	30.07	23.03
		21.41	27.98	21.69	27.35	21.32
		19.90	24.56	19.81	24.93	20.00
		18.40	21.39	18.34	21.41	18.35
		16.92	17.43	16.78	17.40	16.77

			BLACK TAPE		WHITE TAPE	
TRIAL	POSITION	MH (cm)	D	TH (cm)	D	TH (cm)
4	1	25.90	34.50	26.49	34.70	26.67
		24.40	32.34	24.68	32.62	24.90
		22.91	30.39	23.25	30.43	23.28
		21.41	27.95	21.68	27.50	21.41
		19.90	24.83	19.95	25.10	20.09
		18.40	21.48	18.38	21.54	18.40
		16.92	17.46	16.79	12.49	16.80
4	2	25.79	34.39	26.39	34.38	26.38
		24.28	32.29	24.64	32.11	24.50
		22.79	30.16	23.09	30.04	23.01
		21.29	27.80	21.59	27.34	21.31
		19.78	24.44	19.75	24.47	19.77
		18.28	21.28	18.29	21.17	18.24
		16.80	17.27	16.72	17.05	16.64
4	3	25.90	34.44	26.43	34.43	26.43
		24.40	32.27	24.63	32.24	24.60
		22.91	30.33	23.21	30.05	23.02
		21.41	27.98	21.69	27.43	21.37
		19.90	24.58	19.82	24.88	19.97
		18.40	21.41	18.35	21.41	18.35
		16.92	17.43	16.78	17.41	16.77

			BLACK TAPE		WHITE TAPE	
TRAIL	POSITION	MH (cm)	D	TH (cm)	D	TH (cm)
5	1	25.90	34.54	26.52	34.61	26.59
		24.40	32.41	24.74	32.65	24.93
		22.91	30.41	23.26	30.43	23.28
		21.41	27.95	21.68	27.45	21.38
		19.90	24.71	19.89	25.03	20.05
		18.40	21.46	18.37	21.57	18.42
		16.92	17.46	16.79	17.50	16.80
5	2	25.79	34.35	26.35	34.24	26.26
		24.28	32.29	24.64	32.11	24.50
		22.79	30.14	23.08	30.01	22.99
		21.29	27.94	21.67	27.37	21.33
		19.78	24.44	19.75	24.52	19.79
		18.28	21.28	18.29	21.20	18.26
		16.80	17.31	16.74	17.07	16.65
5	3	25.90	34.46	26.45	34.48	26.47
		24.40	32.33	24.67	32.16	24.54
		22.91	30.33	23.21	30.07	23.03
		21.41	27.99	21.70	27.36	21.33
		19.90	24.58	19.82	24.82	19.94
		18.40	21.45	18.36	21.44	18.36
		16.92	17.43	16.78	17.43	16.78

Appendix E

Horizontal Movement Calibration Data

I. FIRST PROCEDURE

DIAL POSITION	NO. OF STEPS	DISTANCE TRAVELLED (x 10^{-3} in)				
		TRIAL 1	TRIAL 2	TRIAL 3	TRIAL 4	AVERAGE
	1	7.7	7.1	7.1	7.8	7.4
MOTOR	2	14.2	15.7	14.9	13.7	14.6
END	3	20.4	20.6	21.0	21.0	20.8
	4	28.2	28.6	28.7	27.8	28.3
	5	34.5	34.2	33.4	34.7	34.2
	6	41.3	40.9	40.9	41.0	41.0
	1	6.0	6.4	6.4	6.8	6.4
	2	14.0	13.6	14.4	14.0	14.0
CENTER	3	21.0	20.7	20.1	20.0	20.45
	4	28.3	28.3	28.1	28.2	28.2
	5	35.7	35.3	35.2	35.2	35.4
	6	40.2	40.7	40.8	40.8	40.6
	1	6.0	6.0	6.0	6.0	6.0
	2	13.0	13.2	14.6	13.8	13.65
GEAR	3	21.0	21.1	19.6	20.2	20.5
END	4	29.5	28.7	28.8	29.0	29.0
	5	34.5	34.6	35.2	34.0	34.6
	6	41.0	39.4	40.8	41.3	40.6

II. SECOND PROCEDURE

NO. OF STEPS	ERROR (x 10^{-3} in)			
	DIAL AT MOTOR END		DIAL AT GEAR END	
	TRAIL 1	TRIAL 2	TRIAL 1	TRIAL2
50		-1.0		0.0
100	-2.1	1.8	-1.3	-0.9
150		0.0		0.0
200	2.0	-0.2	0.0	1.0
250		-0.8		0.0
300	0.2	-1.1	0.5	1.0
350		1.8		0.0
400	-1.2	0.0	1.1	0.0
450		-4.0		-0.8
500	1.1	4.8	-1.5	0.0
550		-2.0		1.0
600	-2.0	-0.2	1.1	-2.8
650		1.0		0.8
700	1.2	-1.0	1.0	0.0
750		2.4		0.7
800	0.0	1.0	1.3	0.0
850		-3.0		0.0
900	-1.9	3.1	2.0	0.0
950		-3.8		0.0
1000	0.9	2.1	1.2	0.0
1500	-0.9	-1.3	1.1	1.8
2000	-1.8	1.1	-0.5	1.0
2500	3.0	-3.8	1.0	1.0
3000	0.0	2.2	0.0	1.5
3500	0.3		0.0	
4000	-2.0		0.0	

Appendix F

Height Measurement Calibration Data Collected

by the Camera with the 50 mm Lens

			BLACK TAPE		WHITE TAPE	
TRIAL	POSITION	MH (mm)	D	TH (cm)	D	TH (cm)
1	1	30.00	114.40	30.03	114.40	30.03
		28.50	103.50	28.48	103.60	28.49
		27.00	91.46	16.95	91.77	26.98
		25.50	78.37	25.45	78.21	25.43
		24.00	63.54	23.94	63.50	23.94
		22.50	47.06	22.47	47.08	22.47
		21.00	28.56	21.02	28.74	21.03
1	2	29.90	113.00	29.82	113.20	29.85
		28.40	102.30	28.32	102.50	28.35
		26.90	90.29	26.80	90.48	26.83
		25.40	76.92	25.29	77.09	25.31
		23.90	62.40	23.84	62.43	23.84
		22.40	45.85	22.37	46.00	22.78
		20.90	27.50	20.94	27.43	20.93
1	3	30.10	114.10	24.99	114.30	30.01
		28.60	103.50	28.48	103.60	28.49
		27.10	91.58	26.96	91.94	27.00
		25.60	78.61	25.47	78.75	25.50
		24.10	64.42	24.03	64.62	24.05
		22.60	48.10	22.56	48.21	22.05
		21.10	30.05	21.13	29.97	21.12

			BLACK TAPE		WHITE TAPE	
TRIAL	POSITION	MH (mm)	D	TH (cm)	D	TH (cm)
2	1	30.00	14.20	30.00	114.30	30.01
		28.50	103.60	28.49	103.60	28.49
		27.00	91.46	26.95	91.60	26.96
		25.50	78.34	25.44	78.23	25.43
		24.00	63.44	23.93	63.55	23.95
		22.50	47.07	22.47	47.05	22.47
		21.00	28.50	21.01	28.63	21.02
2	2	29.90	113.00	29.82	113.00	29.82
		28.40	102.50	28.35	102.40	28.33
		26.90	90.38	26.82	90.47	26.83
		25.40	76.82	25.18	77.16	25.32
		23.90	62.35	23.84	62.57	23.86
		22.40	45.87	22.37	46.02	22.38
		20.90	27.58	20.95	27.54	20.94
2	3	30.10	114.00	29.97	114.30	30.01
		28.60	103.50	28.48	103.60	28.49
		27.10	91.64	26.96	91.97	27.01
		25.60	78.61	25.47	78.78	25.50
		24.10	64.48	24.04	64.54	24.04
		22.60	48.14	22.56	48.20	22.57
		21.10	30.07	21.13	29.97	21.12

			BLACK TAPE		WHITE TAPE	
TRIAL	POSITION	MH (mm)	D	TH (cm)	D	TH (cm)
3	1	30.00	114.30	30.01	114.40	30.03
		28.50	103.60	28.49	103.60	28.49
		27.00	91.50	26.95	91.67	26.97
		25.50	78.32	25.44	78.34	25.44
		24.00	63.52	23.94	63.50	23.94
		22.50	47.00	22.47	47.12	22.47
		21.00	28.56	21.02	78.63	21.02
3	2	29.90	112.80	29.79	113.10	29.84
		28.40	102.30	28.32	102.50	28.35
		26.90	90.30	26.80	90.49	26.83
		25.40	76.79	25.28	77.15	25.32
		23.90	62.25	23.83	62.46	23.85
		22.40	45.71	22.36	46.00	22.38
		20.90	27.40	20.93	27.54	20.94
3	3	30.10	114.00	29.97	114.20	30.00
		28.60	103.50	28.48	103.50	28.48
		27.10	91.65	26.97	91.89	27.00
		25.60	78.63	25.47	78.57	25.47
		24.10	64.38	24.03	64.34	24.02
		22.60	47.96	22.55	48.02	22.55
		21.10	30.11	21.13	29.86	21.12

			BLACK TAPE		WHITE TAPE	
TRIAL	POSITION	MH (mm)	D	TH (cm)	D	TH (cm)
4	1	30.00	114.20	30.00	114.30	30.01
		28.50	103.50	28.48	103.60	28.49
		27.00	91.46	26.95	91.68	26.97
		25.50	78.20	25.43	78.26	25.44
		24.00	63.44	23.93	63.44	23.93
		22.50	46.81	22.45	46.99	22.47
		21.00	28.40	21.01	28.61	21.02
4	2	29.90	112.80	29.79	113.00	24.82
		28.40	102.30	28.32	102.40	28.33
		26.90	90.37	26.82	90.42	26.82
		25.40	76.79	25.28	77.10	25.31
		23.90	62.25	23.83	62.25	23.83
		22.40	45.80	22.37	45.96	22.38
		20.90	27.42	20.93	27.34	20.93
4	3	30.10	114.10	29.99	114.10	29.99
		28.60	103.50	28.48	103.50	28.48
		27.10	92.56	26.96	91.80	26.98
		25.60	78.50	25.46	78.03	25.47
		24.10	64.26	24.02	64.25	24.02
		22.60	47.83	22.53	48.10	22.56
		21.10	29.99	21.12	29.99	21.12

			BLACK TAPE		WHITE TAPE	
TRIAL	POSITION	MH (mm)	D	TH (cm)	D	TH (cm)
5	1	30.00	114.30	30.01	114.40	30.03
		28.50	103.50	28.48	103.50	28.48
		27.00	91.40	26.94	91.63	26.96
		25.50	78.38	25.45	78.26	25.44
		24.00	63.44	23.93	63.40	23.93
		22.50	46.86	22.46	47.06	22.47
		21.00	28.34	21.00	28.66	21.03
5	2	29.90	112.90	29.81	113.00	24.82
		78.40	102.30	28.32	102.40	28.33
		26.90	90.23	26.79	90.34	26.80
		25.40	76.74	25.77	76.97	25.30
		23.90	62.28	23.83	62.31	23.83
		22.40	45.65	22.36	45.94	22.37
		20.90	27.50	20.94	27.39	20.93
5	3	30.10	114.00	29.97	114.10	29.99
		28.60	103.50	28.48	103.50	28.48
		27.10	92.56	26.96	91.89	27.00
		25.60	78.54	25.46	78.64	25.47
		24.10	64.24	24.61	64.33	24.02
		22.60	47.87	22.54	48.02	22.55
		21.10	29.88	21.12	29.90	21.12

Appendix G

Calibration Software

```
//NLIN JOB W.SAS.CLASS=Q.X
/*KEY.Y
/*ROUTE PRINT VM1.Z
OPTIONS LS=80:
TITLE SOIL PROFILER CALIBRATION PROGRAM:
DATA:
INPUT MH D TH:
CARDS:
30.00 114.40 30.03
          :
          :
          :
          :
PROC NLIN:
PARMS K1=n K2=m:
MODEL MH=K1/(K2-D):
DER.K1=1/(K2-D):
DER.K2=-K1/(K2-D)**2:
OUTPUT RESIDUAL=RES1:
PROC NLIN:
PARMS K1=n K2=m K3=k:
MODEL MH=K1/(K2-D)+K3:
DER.K1=1/(K2-D):
DER.K2=-K1/(K2-D)**2:
DER.K3=1:
OUTPUT RESIDUAL=RES2:
PROC PRINT: VAR MH D TH RES1 RES2:
//
```

The calibration software utilizes the VM's Statistical Analysis System (SAS). The program must have a SAS filetype (e.g., filename.SAS.A). To RUN the program the command SUBMIT filename.SAS.A should be executed. The output will come back to the user's READER files which can be accessed by RLOOK or RDR commands and copied into a file by DEPRINT filename.filetype.A command.

The NLIN is a SAS procedure which is called to analyze non-linear models. The letters w, x, y, and z in lines 1 through 3 should be replaced with user's acocunt number, initials, longkey, and userid, respectively. The INPUT line includes the list of variables (MH, D, and TH) in the model whose values are measured and listed in lines below the CARDS line. The PARMS line is used for an intial estimated value (n, m, and k) of the constant parameters k1, k2, and k3. The MODEL line contains the model to be analyzed. The DER lines include the partial derivatives of the model with respect to the constants k1, k2, and k3. The OUTPUT line provides the residuals of the model and the PROC PRINT prints them along with the variables MH, D, and TH.

Appendix H

Soil Data

LEVEL	MH	TH(cm)								
	(cm)	SOIL1	SOIL2	SOIL3	SOIL4	SOIL5	SOIL6	SOIL7	SOIL8	SOIL9
1	20.38	20.36	20.43	20.36	20.34	20.41	20.36	20.39	20.42	20.48
	20.37	20.19	20.22	20.25	20.14	20.21	20.20	20.20	20.21	20.41
	20.36	20.11	28.18	20.17	20.13	20.13	20.16	20.20	20.21	20.30
	20.34	20.15	20.22	20.15	20.16	20.17	20.19	20.18	20.20	20.26
	20.33	20.32	20.32	20.27	20.30	20.30	20.30	20.31	20.38	20.37
2	25.09	25.03	25.12	25.08	25.06	25.12	25.07	25.07	25.11	25.08
	25.03	24.80	24.85	24.92	24.84	24.87	24.90	24.82	24.88	25.01
	24.97	24.68	24.77	24.76	24.77	24.76	24.81	24.75	24.82	24.86
	24.92	27.70	24.77	24.72	24.73	24.74	24.81	24.71	24.81	24.79
	24.86	24.80	24.84	24.77	24.80	24.85	24.89	24.78	24.90	24.86
3	30.09	30.06	30.17	30.05	30.06	30.12	30.05	30.06	30.12	30.15
	30.03	29.80	29.89	29.90	29.88	29.89	29.85	29.80	29.92	30.02
	29.98	29.70	29.80	29.73	29.80	29.77	29.73	29.75	29.85	29.86
	29.92	29.69	29.80	29.73	29.73	29.73	29.70	29.70	29.80	29.80
	29.86	29.79	29.83	29.83	29.79	29.82	29.77	29.79	29.90	29.86

The soil data listed is only the portion used in the statistical analysis (5 points from a total of 43 points along the profile meter). The TH is an average of 3 measurements at each point by the profile meter.

The vita has been removed from the scanned document